The start of a major sea-level rise indicates that ice-sheet expansion in western Norway commenced before the Younger Dryas

Øystein S. Lohne [a*], Stein Bondevik [b], Jan Mangerud [a,c], John Inge Svendsen [a,c]

[a] Department of Earth Science, University of Bergen, Allégt. 41, N-5007 Bergen, Norway
[b] Department of Geology, University of Tromsø, Dramsveien 201, N-9037 Tromsø, Norway
[c] The Bjerknes Centre for Climate Research, Allégt. 55, N-5007 Bergen, Norway

[*] Correspondence to: Øystein S. Lohne, Department of Earth Science, University of Bergen, Allégt. 41, N-5007 Bergen, Norway. Telephone: (47) 55 58 81 12, Fax (47) 55 58 36 60, Email: oystein.lohne@geo.uib.no

Submitted to Quaternary Science Reviews.

Abstract

The relative sea level rose 10 m on Sotra, western Norway, during the Younger Dryas (YD). Based on dating of isolation basins, the transgression started in late Allerød at ~13 110 and ended in late YD at ~11 780 cal yr BP, with an average sea-level rise of ~7 mm yr^{-1}. Between ~11 780 and ~11 560 cal yr BP the relative sea level was stable. Shortly after the YD/Holocene boundary the sea level rapidly fell 37 m at ~23 mm yr^{-1}. The shorelines for the regression minimum in Allerød and the transgression maximum in YD are almost parallel with tilt of 1.2-1.4 m km^{-1}, indicating that no isostatic tilting, and thus neither uplift or depression occurred during the sea-level rise. We conclude that the transgression was caused by a YD ice-sheet re-advance mapped in the same area. This stopped the isostatic uplift and increased the gravitational attraction on the sea elevating the geoid in this area. There may also been a contribution from rising glacio-eustatic sea level. Our results show that the transgression started around 13 110 cal yr BP. Thus, we conclude that the YD ice-sheet advance in western Norway started before the onset of the YD.

1. Introduction

A 9-12 m relative sea-level rise during the Younger Dryas (YD) constitutes a major feature of the Late Weichselian sea-level history of western Norway (Krzywinski and Stabell, 1984; Anundsen, 1985; Lohne et al., 2004). The transgression has been called the YD-transgression (Anundsen, 1985). Numerical simulations carried out in the 1980`s suggested that the transgression was caused by a major (> 50 km) YD ice-sheet readvance (Mangerud, 1977; Fjeldskaar and Kanestrøm, 1980; Anundsen and Fjeldskaar, 1983; Mangerud, 2004). A strong synchronicity between the maximum ice-sheet position (Bondevik and Mangerud, 2002) and the peak of the transgression (Lohne et al., 2004) supports this causative connection. The model indicates that the re-growth of the ice sheet reduced the rebound of the crust and the increased mass of ice also attracted, by gravity, more seawater towards the coast. Together with a at that time postulated eustatic sea-level rise of 10 m during YD (Shepard, 1963), the model simulated a regional transgression in western Norway during the YD. However, more recently Lambeck et al. (2002) postulated that the eustatic sea level was constant during the YD, which implies that this transgression was caused only by the regional components. In order to understand the transgression a better description of its three-dimensional extension and accurate timing is necessary. In this paper we present a well-dated sea-level curve from Sotra, 10 km west of Bergen (Fig. 1), which represents one-step forward in this description.

In the late 1970's a large number of isolation basins were studied at Sotra (Fig. 1) to construct a relative sea-level curve. The lateglacial part of the curve (Krzywinski and Stabell, 1984), was one of the first to document the YD transgression in Western Norway. Many of the basins were analysed in detail both for pollen and diatoms. Nevertheless, the curve has subsequently been revised by correcting the basin elevations for tilt, and by re-interpretation of the chronostratigraphy (Anundsen, 1985; Svendsen and Mangerud, 1987). We have now improved the lateglacial part of this curve by collecting new cores from two of the previously studied basins and by analysing an additional basin. Together these basins record the Allerød regression minimum (lowstand) and the YD transgression maximum (highstand) of the sea level. Many samples of terrestrial plant macrofossils have been dated, and a solid calendar-year chronology for the lateglacial sea-level changes has been established. The

Holocene part of the curve has also been calibrated and re-evaluated (Krzywinski and Stabell, 1978; Stabell and Krzywinski, 1979), and we present a complete curve from Sotra in calendar year time scale.

The possible causes (isostasy, eustasy, gravity) for the transgression would cause different changes in the tilt of the shorelines. Therefore we also constructed the regression minimum shoreline in late Allerød, and the shoreline at the transgression maximum high stand in the late YD. For this we used the new sea-level curve from Sotra, a sea-level curve from Os (Lohne et al., 2004) and the altitude of marine-limit terraces in the area (Fig. 1).

A lateglacial relative sea-level rise has been described from several localities in southwestern Norway. (e.g. Fægri, 1940; Fægri, 1944; Thomsen, 1982; Krzywinski and Stabell, 1984; Anundsen, 1985). It is generally agreed that this is the same sea-level event and the name "YD transgression" is commonly used. In the present paper we therefore use the name "YD transgression", even though the relative sea-level rise sums to have started somewhat before the YD cooling. It should also be mentioned that the term is used to signify a vertical change of the shoreline, i.e. a relative sea-level rise.

2. Methods

Our main strategy in reconstructing former sea-level changes has been to use the so-called isolation basin method (Hafsten, 1960; Svendsen and Mangerud, 1987). The basis of this method is that stratigraphic boundary between marine and lacustrine sediments in lakes correspond with the isolation of the lake from the sea, i.e. the time when the sea level was at the level of the outlet threshold of the lake basin. Such a sedimentary boundary, where marine sediments are overlain by lacustrine, is called an *isolation contact*. When the relative sea-level rise and inundate a lake, marine sediments will start to accumulate above the lacustrine sediments, and the sediment boundary is called the *ingression contact*. The isolation and ingression contacts are considered to reflect the period when the outlet threshold corresponds with the high tide level.

The basins investigated in the present study were levelled to a survey control point that refers to the national datum level (NN1954). At a tide gauge in the city of Bergen the NN1954-datum lies 1.5 cm above the mean tide level (Olav Vestøl,

Norwegian Mapping Authority, pers. comm. 2004). Uncertainties connected to the levelling and the datum level, are in the order of cm and are in this context negligible. In the original Sotra study (Krzywinski and Stabell, 1984) the threshold elevation of the basins were measured from the upper growth limit of the brown algae *Fucus vesiculosus* (Berge et al., 1978) that occur close to the mean tide level. We apply an uncertainty of ±0.5 m for these measurements that are related to the site specific determination of the *Fucus vesiculosus* upper growth limit and to the relation of the growth limit and the mean tide level. All basins have a bedrock threshold that has undergone negligible erosion after isolation from the sea. Nevertheless, some of the basins thresholds have been changed by human activity (local roads, farming etc.), and an additional uncertainty of ±0.5 m has therefore been added for these basins.

A Russian peat corer was used to map the deposits across the basins along transects. Based on this mapping we chose the location for the main core used for further laboratory analyses. These main cores were either sampled with a 110 mm piston corer or a 110 mm Russian peat corer.

In the laboratory we measured loss on ignition and magnetic susceptibility of the cores. Samples of constant volume (1 cm^3) were dried overnight at a temperature of 105°C and than heated to 550°C for 1 hour. The loss on ignition was calculated as a weight percentage of the dried sample. Magnetic susceptibility and density were analysed using a GEOTEK Multi-Sensor Core Logger.

Diatom slides were prepared as smear slides and mounted with Mountex (RI=1.67). At least 300 diatom valves were identified (Hustedt, 1930, 1930-66, 1957; Hendey, 1964; Krammer and Lange-Bertalot, 1986, 1988, 1991a, 1991b; Witkowski et al., 2000) and counted on each slide, and the diatom distribution were plotted as percentages grouped to the salinity preferences (Table 1) deduced empirically (de Wolf, 1982; Denys, 1991/2).

Radiocarbon dating was performed on terrestrial plant macrofossils in order to avoid hardwater effects and marine reservoir age problems (Mangerud and Gulliksen, 1975; Barnekow et al., 1998). The plant fragments were carefully picked from sieved material larger than 250 μm. In order to establish a firm chronology on a calendar year time scale many samples were ^{14}C dated.

The conversion to calendar year ages were done by analysing series of dates with the sequence function in the calibration software OxCal v3.10 (Bronk Ramsey, 2005), and the calibration curve INTCAL04 (Reimer et al., 2004) This method takes advantage of Bayesian statistics, which allows prior information to be incorporated into the calibration process. Applied to stratigraphic sequences this mean that ages have to increase with depth (Blockley et al., 2004). The method generates what is called prior and posterior probability distributions of ages for each sample. The prior (unconstrained) distribution simply is the probability curve for the calibrated age range for each single ^{14}C date. The posterior (constrained) distribution is the result of constraining the calibrated probability distributions to ensure that all ages increase with depth. The agreement index (A) expresses the convergence between the prior and posterior distributions. An A-index is calculated for the entire sequence and for each individual date and can be used as a measure of the reliability of the imposed age model and for each date (Walker et al., 2003; Blockley et al., 2004). The 'sequence function' in OxCal treat the radiocarbon dates as evenly distributed in the sequence, but has a possibility for separating segments of better dated intervals by so-called 'boundaries'. The dates in our records are unevenly distributed (concentrated close to the sea-level events that we want to date), and we present models with boundaries. A test with unbound models obtained only slightly different results (figure not shown). The results obtained by the sequence function are reported as calendar year intervals (used in tables and figures) or as weighted averages of the posterior probability distribution (used in the text).

The occurrence of the Vedde Ash Bed (Mangerud et al., 1984) in almost all our cores was a great help, both for correlation in the field and as a calendar year date of 11 980 ± 80 ice core (GRIP) yr BP (Grönvold et al., 1995). When necessary the ash layer was identified by counting ash particles larger than 63 μm under a stereomicroscope sieved from samples of constant volume (1 cm^3). We also took advantage of the distinct rise in *Betula* (birch) pollen close to the YD-Holocene boundary (Kristiansen et al., 1988; Paus, 1989; Berglund et al., 1994; Bondevik and Mangerud, 2002) as a stratigraphical marker. At Os (Fig. 1) the *Betula* rise is found stratigraphically slightly (a few cm) above the YD-Holocene boundary (Lohne et al., 2004).

3. The investigated basins

3.1 Gardatjønn (39.3±0.5 m a.s.l.)

Gardatjønn is a small (75x75 m) lake located in the central part of Sotra (Figure 1). The lake has a drainage/surface area ratio of 16.3/0.6 ha. A road has been built across the threshold area which has disturbed the former threshold of the lake. The given altitude of 39.3 m a.s.l. was measured on the bedrock surface in the outlet creek, and we believe it could not have been higher because tree trunks are rooted along the lakeshores. The thickest lateglacial deposits were located in a small area within the deepest part of the lake, where the analysed piston core (505-27) was obtained at 60°17.68′N – 05°05.20′E.

The base of the core (Fig. 2) consists of a diamicton, and is interpreted as a till. The units above the till (1206-1187 cm) consist of a transitional silt clay unit and silty gyttja unit where the organic content gradually increases upwards (Fig. 2). At 1187 cm the lithology changes sharply to brownish grey gyttja silt. Across this boundary there is also recorded a distinct change in the LOI, magnetic susceptibility and the density. The dates and the lithostratigraphy indicate that this boundary represents the Allerød/YD transition. The Vedde Ash Bed is present at a depth of 1178 cm and is recognised as a thin, hardly visible lamina. A distinct gravelly layer occurs at 1167 cm. At 1161-1158 cm, there is a distinct but gradual transition to the overlying dark brown (Holocene) gyttja (Fig. 2).

The diatom record shows that nearly all the deposit in the basin are lake deposits, except for an eight-cm interval of marine/brackish sediments close to the YD/Holocene transition. This interval is dominated by marine- and brackish-water diatoms - both planktonic and benthic species (Fig. 2 & Appendix A). However, there are also many valves of the euryhaline *Fragilaria*-sp. diatom in this layer, a species often associated with isolation contacts (Stabell, 1985). This may indicate that only spring tides reached above the bedrock threshold of the lake at this time. Other lakes at Sotra at a slightly higher elevation (e.g. Førekleivsvatn at 41.3 m a.s.l. Table 4) do not show any trace of a marine incursion. We thus consider the threshold at Gardatjønn to be within 0-2 m below the high tide sea level when the eight-cm interval was deposited.

^{14}C ages show that the marine interval is centred on the 10 000 ^{14}C yr BP plateau. The Vedde Ash Bed occurs at 1178 cm - nine cm below the first occurrence of

marine diatoms, and the rise of *Betula* (birch) - pollen was found 2 cm below (at 1163 cm) the upper boundary of the marine interval (Fig. 2). We used Bayesian analysis on the 15 radiocarbon ages from the core, including the age of the Vedde Ash Bed, and provide the age of ca 11 780 cal yr BP for the lower boundary of the marine interval (ingression contact) and ca 11 560 cal yr BP for the upper boundary, the isolation contact (Table 2). The highstand sea level in Gardatjønn thus had duration of about 220 years, or between 80-360 years (1σ) according to the Bayesian results (Fig. 3), and thus, occurred from the very late YD until the early Preboreal (slightly after the *Betula* rise).

3.2 Hamravatn (29.1±0.5 m a.s.l. – tilt adjusted to 31.3±1.4 m a.s.l.)

Hamravatn is a small (50x250 m) lake in the south western part of the island Sotra (Fig. 1), with drainage/surface area ratio of 41.3/0.6 ha. The stratigraphy of the basin was originally investigated by Krzywinski and Stabell (1984). We re-examined the deposits in the lake using a Russian peat corer, and collected two overlapping cores with a piston corer from the central and deepest part of the lake at 60° 12,41′N – 05° 05,13′E. The new cores can easily be correlated by lithology with the core presented in figure 14 in Krzywinski and Stabell (1984). However, our radiocarbon ages are about 200-300 years younger than Krzywinski and Stabell's (1984) three ^{14}C ages from corresponding stratigraphical depth. But as their samples are of bulk sediments and the deposits have low carbon content (LOI values are low), we regard our dates on terrestrial plant fragments as much more accurate. The lithostratigraphy of our core is described in Fig. 4, and it represents deposits from the deglaciation of the area (prior to 12 270 ^{14}C BP) to the early Holocene. The sediments and diatoms reflect a depositionary environmental succession from glacio-marine – marine – lacustrine (Allerød) – marine (YD) – lacustrine (Holocene).

Our main focus has been the lower lacustrine phase (Fig. 4), which coincides with the deposition of the silty gyttja (1312-1290 cm), and which shows that the relative sea level was below the threshold for a period during the Allerød. The lower boundary constitutes a sharp sedimentary change from homogenous greyish silt to finely laminated algae gyttja. The diatoms show a sharp transition from marine to lacustrine flora across this boundary, and verify the inferred position of the isolation contact. Marine diatoms occur again in the sediments just above the upper boundary of the silty gyttja. The ingression contact has been interpreted to coincide with the

lithological boundary at 1290 cm, even though species grouped as freshwater indicators occur above this boundary. These are mainly euryhaline *Fragilaria* species (Appendix B) that often are found close to isolation and ingression contacts (Stabell, 1985).

From the upper part of the lacustrine gyttja and in the succeeding marine silt we dated five levels; the sample at the ingression contact between 1290 and 1292 cm has an age of 11 080 ± 50 ^{14}C yr BP. However, from the first isolation of the lake we could only find material for one sample, dated to 12 090 ± 60 ^{14}C yr BP (Fig. 4). The Bayesian analysis of the sequence of dates and the Vedde Ash Bed from Hamravatn (not shown) estimates the age of the isolation contact (A) to ca 13 920 cal yr BP and the ingression contact (B) to ca 12 950 cal yr BP (Table 3). The model obtained an agreement index of 99.2 %.

3.3 Sekkingstadtjønn (24.3±0.5 m a.s.l. – tilt adjusted 29.6±1.1 m a.s.l.)

Sekkingstadtjønn is a small (100x150 m) lake situated at the western part of the island of Sotra (Fig. 1). A core from the deepest part of the lake at 60° 21,00′N – 04° 59,66′E, revealed a zone of densely laminated sediments in a zone below the Vedde Ash Bed (Fig. 5). Such laminations are characteristic for brackish sediments deposited during isolation of a basin (Kaland, 1984; Svendsen and Mangerud, 1987), and we therefore considered that this laminated zone could reflect the regression minimum in Allerød, even though that Krzywinski and Stabell (1984) reported that no traces of lacustrine or brackish sediment were found in the lateglacial sequence.

In the two parallel Russian cores (1 m long) obtained from the deepest part of the lake the laminated brownish silty gyttja is about 10 cm thick with olive grey and reddish brown laminas (Fig. 5). The LOI values are distinctly higher than below and above. The lower boundary of the laminated zone is sharp regarding lithology, colour and LOI. The diatoms show similar pattern with a sharp transition from a marine dominated flora to predominantly lacustrine/brackish species at the base of the unit (Fig. 5, Appendix C). According to the diatoms, the lower boundary (at 1303 cm in Fig 7) represents the time when the sea level fell below the threshold so that seawater only occasionally, at very high tides, flowed into the basin. Four cm higher up in the laminated zone (at 1299 cm), about 90 % of the diatom flora belong to lacustrine/brackish species and probably seawater entered the basin only at extreme tide episodes and/or storm surges. Above 1299 cm the diatom flora is gradually replaced by

marine species, and at a depth of 1289 cm only scattered freshwater diatoms occur. Because of the gradual change it is difficult to place the boundary exactly when the basin was submerged during the following transgression. In general the signature of the diatoms at such contacts varies between basins due to the rate of sea-level change, exposure to open marine waters, freshwater input, and size and bathymetry of the basin. Sekkingstadtjønn has limited freshwater input from a small (16.1 ha) drainage area. We therefore suggests that the increasing amount of marine diatoms from 1299 cm and upwards reflects increasing numbers of spring tides into the basin, and that daily tides rose above the threshold of Sekkingstadtjønn first at the time corresponding to 1291 cm where marine diatoms became dominant (>90%). The gradual increase of marine diatoms may suggest that relative sea-level rise at this time was somewhat slower than the sea-level fall at the start of this brackish zone. The contacts below and above the brackish zone (at 1303 and 1291 cm) are hereafter called isolation and ingression contacts respectively, even though the lake was not entirely isolated from the sea during this time span. The main point is that the brackish deposit demonstrates that the threshold of Sekkingstadtjønn precisely defines the sea level at the lateglacial regression minimum, and that the interpreted position of the ingression contact provides a minimum age for the start of the YD-transgression.

In order to date the regression minimum accurately we dated terrestrial plant macrofossils at nearly every cm throughout the laminated unit (Fig. 5, Table 2). The sequence of radiocarbon dates and the Vedde Ash Bed was analysed using the Bayesian method (Fig. 6). The model estimate an age of ca 13 610 cal yr BP for the first isolation contact and ca 13 110 cal yr BP for the subsequent ingression contact (Table 3). The brackish phase, and thus the sea-level lowstand (regression minimum), lasted about 500 years in Sekkingstadtjønn, or between 270-660 years (1σ) according to the Bayesian results (Fig. 6).

4. The sea-level curve from Sotra

The focus of the present study is the lateglacial sea-level history. Nevertheless, we have also included radiocarbon ages of Holocene age from available isolation and ingression contacts on Sotra (Table 4) into a complete late- and postglacial sea-level curve (Fig. 7).

The basins at Sotra are located at different isobases (Fig. 1). In order to combine them all into one sea-level curve the altitude of the basins need to be adjusted for differential isostatic uplift. The sea-level curve has been constructed for an isobase through Gardatjønn with a direction of 351±4° (see below). The tilt gradient varies trough time and the individual sea-level index points for the lateglacial period have been adjusted according to shoreline gradients determined in the present study (see below) and the Holocene points according to the shoreline gradients from the diagram of Kaland (1984). The basins are found along the isobases, in a distance of about 30 km (Fig. 1), which due to uncertainties of the isobase directions introduces uncertainties to the projected position at the projection plane and therefore also uncertainties in the tilt corrections.

4.1 Lateglacial and early Holocene sea-level changes

The stratigraphy and the ^{14}C ages from the three basins Gardatjønn, Sekkingstadtjønn and Hamravatn precisely define the YD transgression. The Allerød regression minimum is determined in Sekkingstadtjønn, at 29.6 m a.s.l., which also indicates a more or less stable relative sea level for about 500 years between ca 13 610 and ca 13 110 cal yr BP. After this relative sea level started to rise and reached above the 2-m-higher Hamravatn at ca 12 950 cal yr BP. Thus it is evident that the YD transgression started before the onset of the YD period usually dated to 13 000-12 800 cal yr BP (e.g. Hughen et al., 2000). The marine/brackish sediments, dated between ca 11 760 and ca 11 560 cal yr BP in Gardatjønn represent the peak of the YD transgression at 39.3 m a.s.l. In the about 2-m-higher Førekleivsvatn there is only lacustrine deposits (Krzywinski and Stabell, 1984), supporting the interpretation that sea level did not reach much higher than Gardatjønn (Table 4, Fig. 7). The sea-level curve shows that the amplitude of 9.7 ± 1.6 m for the YD transgression at Sotra, and an average sea-level rise during the transgression of 7 mm yr^{-1}.

After the YD the relative sea level fell rapidly from 40 m a.s.l. to below 5 m a.s.l. in 1500 years (Fig. 7). This major regression started after the rise in *Betula* sp. (birch) pollen, and was dated to about ca 11 560 cal yr BP, at Gardatjønn. Also the pollen diagrams (Krzywinski and Stabell, 1984) from basins slightly below Gardatjønn (Kvernavatn 38.9 m a.s.l., Klæsvatn 34.9 m a.s.l., Hamravatn 31.3 m a.s.l.) supports that the regression started after the first distinct *Betula* rise.

4.2 Holocene

The re-evaluation of the basins that were affected by the Holocene sea-level changes revealed that several of the sediment sequences had hiati, massive sand beds, and chaotic sediments, indicating that these were disturbed. These features have later been shown to be characteristic for basins inundated by the Storegga tsunami (Bondevik et al., 1997a; Bondevik et al., 1997b). The tsunami occurred about 7300 ^{14}C yr BP, or ca 8150 cal yr BP (Bondevik et al., 2005), and was the result of the giant Storegga slide offshore Norway (Haflidason et al., 2004).

Tsunami deposits have been found in isolation basins both below and above the shoreline of that time. Near Sotra the tsunami had a run-up of at least 3-5m (Bondevik et al., 1997a) and one would expect it inundated most of the basins that were isolated after ~11 000 cal yr BP. When constructing the revised sea-level curve, we have excluded basins where the relevant part of the stratigraphical sequence obviously was disturbed by the Storegga tsunami (Table 4). Judged by the available descriptions (Indrelid et al., 1976; Berge et al., 1978; Stabell and Krzywinski, 1978), the remaining basins used to date the sea-level curve seem undisturbed near the isolation and ingression contacts. However, the sediment descriptions are sparse, and during the previous investigation the Storegga tsunami was yet not recognized and it is therefore quite possible that traces of this event has been overlooked. According to our judgement two parts of the curve (Fig. 7) are uncertain for this reason; the low stand at 9500 and the following relative sea-level rise, the mid-Holocene, so-called Tapes transgression, from 9500 and until the tsunami occurred at about 8 150 cal yr BP.

The low stand is defined by the lacustrine sequence in Trollabotn with a threshold of 4.8 m a.s.l. (Loc. 15, Fig. 1, and Table 4). However, the upper boundary of the 35 cm thick lacustrine is sharp, and may represent an erosional break (tsunami?) Anyhow the lacustrine sequence representing enough time (510-1180 yrs in the 1σ interval, Table 4) for sea level to fall significantly lower. Lacustrine sediments are not reported in lower basins but such deposits could have been removed by the tsunami, or thick tsunami sand beds might have prevented deeper coring. We are therefore open for the possibility that the early Holocene regression minimum was below 5 m.

The tsunami causes problems for reconstructing the relative sea-level rise during the Tapes transgression (Bondevik et al., 1997a; Bondevik et al., 1998). Before

the AMS method was introduced bulk samples of the lacustrine sediment just below the ingression contact was dated. If the tsunami had eroded into this unit, the dates would yield too old age. Two "ingression dates" (locs. 10 and 15, Table 4) have been omitted because massive sand beds indicating erosion were described on this boundary (Indrelid et al., 1976; Berge et al., 1978; Stabell and Krzywinski, 1978). In the other basins (locs. 9, 12 and 13, Table 4) the descriptions do not indicate erosion, and these dates are plotted on the curve. However, conservatively we accept the possibility for erosion even here, and we have therefore indicated an alternative curve showing a slower transgression than given by these dates (Fig. 7).

Stabell and Krzywinski (1979) interpreted thin horizons of greenish algae gyttja in two different basins to represent the maximum of the Tapes transgression (locs. 11 and 16, Table 4). The dates of these episodes deviate by more than 1300 ^{14}C yr. The dates could indicate a long duration of the maximum, or alternatively they could be explained by the large (8 km) west to east distance between the basins (Stabell and Krzywinski, 1979), and thus that they show the metachronous transgression maximum (Kaland, 1984). However, the oldest of these dates (loc. 11, Storevatn) is of Storegga tsunami age, and as chaotic sediments occur frequently in the basin (Berge et al., 1978), this date is currently rejected. The date from basin no. 16 (Torkevikstjønn) is too young to be affected by the Storegga tsunami and we conclude it dates the maximum level of the Tapes transgression to ~6900 cal yr BP (Stabell and Krzywinski, 1978). The last 7000 years is characterised by a gradually lowering of the relative sea level to the present level, reflecting a slow but continues uplift.

5. The YD transgression and its causes

Relative sea-level changes at a locality can be caused by a number of processes that for simplicity can be grouped in (1) vertical movements of the crust (tectonic, glacio- and hydro isostasy) and (2) vertical movements of the sea level (glacio-eustasy and changes in the geoid), both relative to the centre of the Earth.

1. In general Scandinavia experienced emergence during the deglaciation, due to the strong glacio-isostatic uplift. The amount of glacio-isostatic response is linked to ice thickness, and the uplift will produce tilted shorelines, rising towards the former ice centre. Hydro isostasy will influence in the same

direction regarding the tilting, but due to increased water loading along the coast relative to the land. The isostatic deformation of the crust has mainly been in the form of flexure, but there may also have been faulting caused by the increased crustal stress (Gudmundsson, 1999; Anda et al., 2002). However, because of sparse sediment cover in western Norway it is difficult to identify any fault movements and presently no positive evidence for late- and post-glacial faults exits in the area (Olesen et al., 2004). On the contrary, the linear outline of the YD shoreline (see section 5.2) indicates that any vertical faults were minor, and this is not considered further.

2. The dominating vertical eustatic movement during deglaciation was the sea-level rise due to melting of the Earths ice sheets, but also the gravitational attraction between the seawater and the changing land-based masses (ice sheet and land) was important. For the small area we analyse, all the eustatic movements can be regarded as movements of a horizontal surface.

In this section we will describe the geographical extension of the YD transgression (5.1), describe and analyse the geometry of the mid-Allerød and late-YD shorelines (formed before and after the YD transgression, respectively) (5.2), and outline the local influence of the glacio eustatic sea-level change during the YD transgression. Isostatic modelling is planned for a future co-operative study, where the sea-level data will be utilized.

5.1 The geographical extensions of the YD transgression and YD ice-sheet expansion

The YD transgression has been documented several places on the south-western coast of Norway between Stavanger and Bergen (review of Anundsen, 1985; Lohne et al., 2004; this study), (Fig. 1 & Fig. 8). To the north of Bergen and to the south of Stavanger, relative sea level fell during the YD. These regional differences appear on the isobase map where the YD isobase cross the Allerød isobase north of Bergen (in Nordfjord) and south of Stavanger, as illustrated by the 60 m isobase in Fig. 8.

The same part of the coast that was transgressed in YD also experienced the major YD ice-sheet readvance. The magnitude of a glacier advance is often difficult to determine because glacial erosion removes all older deposits during advance. In the Bergen area the readvance has been mapped to be 40 km (Mangerud, 1977, 1980;

Andersen et al., 1995; Mangerud, 2004). In Fig. 8 we have shaded the area where the YD ice sheet re-advanced beyond the location of the 12 ka ^{14}C BP ice-sheet margin, which indicates the area with the largest YD readvance. According to these criteria the major readvance occurred along the western and southern coast of Norway from Nordfjord to Langesund (Fig. 8). This is about the same area where relative sea level rose during the transgression, and it is in accordance with the proposed explanation that the glacier advance caused the YD transgression.

5.2 Were there isostatic movements during the YD transgression?

The degree of tilting of the shorelines is a sensitive indicator for the cause of relative sea-level changes (Fig. 9). Such tilting is a response to glacio-isostatic uplift that produces shorelines that rise towards the former ice centre. If the transgression resulted from isostatic subsidence of the crust, caused by the YD ice-sheet re-expansion, it should be shown as an increase in tilt between the Allerød shoreline and the YD shoreline (Fig. 9D). On the other hand, if the Allerød shoreline has a steeper gradient than the YD shoreline then the crust continued to rise through the transgression period (Fig. 9B).

The Allerød regression minimum shoreline and the YD transgression maximum shoreline are reconstructed perpendicular to the isobase direction, and should therefore show the maximum tilt. We use three data sets; the isolation basins from Sotra (this study) and Os (Lohne et al., 2004) and marine terraces connected with the moraines formed in the late YD (Aarseth and Mangerud, 1974; Bondevik and Mangerud, 2002), i.e. concurrently with the YD transgression maximum.

We first adjusted the reported altitudes to mean sea level. The marine diatoms from the isolation basins record the high tide level and threshold altitudes are therefore adjusted downwards by the present tidal amplitude in Bergen of 0.85m (Tidevannstabeller, 1998). The marine terraces have not been re-surveyed by us. We use the reported altitudes were measured by different investigators during 100 years, giving some uncertainties related to the measuring technique and reference datum. However, how these terraces relate to the sea level at time of formation may introduce a larger uncertainty. In northern Norway the distal parts of recent delta plains lie about 1.5-3m below mean sea level (Corner, 1980). Adjusted for the different tide amplitude (Bergen 0.85 m, Tromsø 1.60 m) the similar number for the Bergen area should be 0.75-1.5 m

below mean sea level. The marine terraces are therefore adjusted upwards by 1m and are considered to show the mean sea level within ± 1m.

In order to construct the shoreline it is further postulated that (1) the direction of the isobases is known, (2) the isobases are parallel within the area and (3) the directions of the isobases have not changed during the time of formation of the relevant shorelines (Svendsen and Mangerud, 1987). These points are discussed below.

1. Aarseth & Mangerud (1974) and Anundsen (1985) estimated the direction of the YD isobases to 347º and 349º respectively, based on the mentioned YD terraces. However, we applied a simple linear trend surface analysis to the basin and terrace data (Davis, 1986) and the best fit of the observations between Herdla to the north and Hagen to the south (Fig. 1) show a slightly more northerly (351º) direction. The plane fits the observations well (R^2= 0.9935), with individual deviations less than 2 m. If we use a determination coefficient better than 0.99, the direction will be 351± 4º (Fig. 10).
2. The isobases are certainly not parallel over long distances (Svendsen and Mangerud, 1987). However, for the restricted area considered in the present study (about 60 km N-S) the isobases can be considered parallel, and any possible error is minor compared to other sources of error.
3. The altitude of the Allerød regression minimum is identified only at two locations in our area and the isobase direction cannot be determined. Therefore any change in direction from Allerød to YD cannot be detected either. However, earlier studies indicate only minor changes of the isobase directions in this area for the entire late- and postglacial period (Kaland, 1984; Anundsen, 1985). As a test we have calculated isobases for the Allerød regression minimum and YD transgression maximum for a larger area in western Norway. This will give mean directions that certainly can deviate from the local directions. Observations from Stavanger, Yrkje, Tau, Os and Sotra (Thomsen, 1982; Anundsen, 1985; Flatekval, 1991; Lohne et al., 2004; this study), where both the Allerød regression minimum and the YD transgression maximum shoreline points are fairly well constrained, have been fitted to linear trend surfaces. The best-fit result defines planes where the directions the Allerød and YD isobases differ by only 2º, and thus indicates

none or only a minor change. We therefore consider the Allerød and YD isobases as parallel.

The resulting shorelines for the Bergen area are shown in Fig. 11. The YD shoreline is plotted as a linear regression line after the observations are projected into the projection plane, indicating a tilt of the YD-shoreline of 1.33 m/km (Fig. 11). The Allerød shoreline, only defined by two points, has a gradient of 1.30 m/km. However, the shoreline tilt is sensitive to the direction of the isobases (Fig. 10) because the observations are spread out along the isobases. Small deviations in direction affect both the absolute values and the ratio between the Allerød and YD shoreline gradients. Within the isobase direction interval defined above (351± 4º), the Allerød shoreline gradients vary between 1.21-1.40 m km^{-1} and the YD shoreline between 1.21-1.47 m km^{-1}(Fig. 10). The differences are small, and for the time being we regard the Allerød and YD shorelines parallel with gradient of 1.2-1.4 m km^{-1}.

The YD shoreline has been interpreted to have a curvilinear concave shape both in the Bergen area (Anundsen, 1985) and in the northern part of Western Norway (Svendsen and Mangerud, 1987). As discussed above we found that the observations in the Bergen area fit a straight line although a second order polynomial regression of the YD-TM observations obtained an slightly better fit (R^2: 0.9938 vs. 0.9935). However, the observations in this area are concentrated in a narrow zone between the coast and the YD ice sheet and the shorelines are therefore only 30-40 km long (Fig. 11) and curving might be difficult to detect. The shoreline diagram of Svendsen & Mangerud (1987), on the other hand, covers about 175 km and the curvilinear shape is therefore better constrained in that area. Model experiments suggest that the YD shoreline is curvilinear in Western Norway (Fjeldskaar and Kanestrøm, 1981).

The shoreline diagram shows that there was no tilted uplift between mid Allerød and late YD, if anything it seems rather opposite, namely that the YD shoreline is slightly steeper than the Allerød. This indicates that the isostatic rebound ceased during this time span. This can be explained by an increased load by a major ice-sheet expansion (see 5.1). However, as the tilted isostatic movement was not distinctly reversed the transgression must have been caused by a eustatic sea-level rise.

5.3 Influence of the glacio-eustatic sea-level change

A main factor in the lateglacial and Early Holocene sea-level history is the melting of land-based ice. Sea-level curves from so-called far field sites (relative to the ice sheet) estimates the sea-level rise caused by the melting to 120-130 m from full glacial to interglacial conditions (e.g. Lambeck et al., 2002; Peltier, 2004). In Fig. 12 two versions of glacio eustatic sea-level curves are plotted together with the relative sea-level curve from Sotra. There is a main difference between the plotted curves during the YD (Fig. 12), which may be important for the interpretation of the causes of the YD transgression. A "residual" curve has been calculated by subtracting the glacio eustatic sea-level curve from the Sotra curve, and shows the vertical movements of the relative sea level at Sotra that not can be explained by the glacio eustatic sea-level variations. The movement shown by the residual curve is an uplift of about 130m since the deglaciation of the area, mainly caused by glacio-isostatic rebound. However, during the period of the YD transgression both residual curves changed distinctly (Fig. 12). The residual curve based on Peltier (2004) flattens for a short period, whereas the curve based on Lambeck (2002) shows a reversing by 6 m. (Fig. 12). The distinct change in the "residual" curve indicates that the YD transgression at least partly was caused by changes in the regional effects (isostasy and/or geoidal eustasy). According to model experiments the regional geoidal sea level would rise 4-7 m due to an YD ice-sheet advance of 40 km (Fjeldskaar and Kanestrøm, 1980). Accounting for this the curve based on Lambeck (2002) indicates more or less isostatic stillstand during the YD, and the curve based on Peltier (2004) indicates distinct isostatic uplift during the YD. If we accept that the isostatic uplift halted as concluded above (section 5.2) then the residual curve based on Lambecks sea-level curve (black continues), with a stop in glacio sea-level rise during YD, is most compatible with our results. The blue dotted residual curve in Fig. 12 would indicate a distinct uplift, which should be shown in tilting of the shoreline.

6. Did the ice-sheet re-advance start during the Allerød?

The relative sea-level curve from Sotra estimates the YD transgression to start about 13 110 cal yr BP. The dates show that the transgression started 100-300 years before the Allerød/YD transition (13 000-12 800 cal. yr BP). The implication is that the load on

the crust increased before the onset of the YD, suggesting that the ice growth commenced well before the YD cooling. However, the ice sheet reached its maximum position in the very late YD, indicating that the advance continued from Allerød and throughout YD.

In the North Atlantic region the Bølling-Allerød interstadial has been inferred to have been warmest in the first part followed by a gradual cooling until the abrupt climatic deterioration at the Allerød/YD transition (e.g. Grootes et al., 1993; e.g. Coope and Lemdahl, 1995). In western Norway the transition has been reconstructed by biotic proxies to a decrease of only about 1-2°C in July temperature (Birks et al., 2004), which is a relative small change compared to the rest of north-west Europe where reconstructions indicate a drop of 3-5°C (e.g. Coope et al., 1998) . This small change is probably a result of relatively cool temperatures during Bølling/Allerød in western Norway (Birks et al., 2004). It is evident that many cirque glaciers survived throughout the Allerød even at low elevations (Larsen et al., 1998), and ice-wedge casts were formed during YD at site close to the sea level (Mangerud, 1987), showing that the climate was suitable for glacial activity throughout the lateglacial in western Norway. Possibly the ice-sheet expansion during the Bølling/Allerød was triggered by increased precipitation. Warmer sea-surface temperatures and less sea-ice cover in the sea west of Norway may favour higher precipitation during the Bølling/Allerød (Koç et al., 1993; Klitgaard-Kristensen et al., 2001) compared to the YD. But, even though the YD sea-surface temperature was considerably lower and the sea-ice cover was more extensive, there was still seasonable open water and possibly Atlantic water flowed northwards along the coast of Norway (Birks et al., 2004), showing that moisture was available also during the YD. Certainly reduced summer melting, also contributed to the ice-sheet expansion. We conclude that the critical temperature and moisture threshold that would trigger ice-sheet expansion in western Norway was reached sometimes during the gradual cooling in Bølling/Allerød, before ~13 110 cal years BP, and that the climatic conditions were suitable for ice-sheet expansion throughout the late AL and YD.

7. Conclusions

1. The well-dated relative sea-level curve from Sotra precisely defines the amplitude of the YD transgression in western Norway to be 10 m.

2. The transgression in fact started in Allerød at around ~13 110 cal years BP, 200-300 years before the Allerød/YD transition.
3. The YD transgression culminated very late in the YD and the maximum sea-level stand occurred completely within the 10 000 ^{14}C yr BP plateau. The sea level remained at the high stand into the onset of the Holocene, just after the rise in *Betula* pollen.
4. The timing of the transgression indicates an increased load by an expanding ice sheet before the YD stadial.
5. The sea-level observations for the marine limit formed in late YD, indicates an isobase direction of 351 ± 4º for the Bergen area.
6. The shorelines for the regression minimum in Allerød and the transgression maximum in YD are almost equally tilted, 1.2-1.4 m km^{-1}. This suggests that no or minor isostatic uplift or subsidence occurred during the transgression. The relative sea-level rise was mainly caused by a change in the geoid from the increased gravitational attraction by the growing ice sheet.

Acknowledgement

We are grateful to the following for their contributions to the study: to Aage Paus that conducted the pollen analysis from Gardatjønn; to Herbjørn Heggen for assistance during fieldwork at Gardatjønn; to Haflidi Haflidason for assisting with the Multi-Sensor Core Logger; to Tomasz Goslar that conducted the radiocarbon analysis; and to Bjørg Risebrobakken for reading and improving the manuscript. Financial support was provided by The Norwegian Research Council, grant no 148765/720.

References

Anda, E., Blikra, L.H. and Braathen, A., 2002. The Berill Fault - first evidence of neotectonic faulting in southern Norway. Norwegian Journal of Geology 82, 175-182.

Andersen, B.G., Mangerud, J., Sørensen, R., Reite, A., Sveian, H., Thoresen, M. and Bergstrøm, B., 1995. Younger Dryas ice-marginal deposits in Norway. Quaternary International 28, 147-169.

Anundsen, K., 1985. Changes in shore-level and ice-front position in Late Weichsel and Holocene, southern Norway. Norsk geografisk Tidsskrift 39, 205-225.

Anundsen, K. and Fjeldskaar, W., 1983. Observed and theoretical Late Weichselian shore level changes related to glacier oscillations at Yrkje, southwest Norway. In: H. Schroeder-Lanz (Ed.), Late- and Postglacial Oscillations of glaciers: Glacial and periglacial forms. A. A. Balkema, Rotterdam, 133-170.

Barnekow, L., Possnert, G. and Sandgren, P., 1998. AMS C-14 chronologies of Holocene lake sediments in the Abisko area, northern Sweden - a comparison between dated bulk sediment and macrofossil samples. GFF 120, 59-67.

Berge, J., Bostwick, L.G., Krzywinski, K., Myhre, B., Stabell, B. and Ågotnes, A., 1978. Ilandføring av olje på Sotra. De arkeologiske undersøkelser 1977. Vindenes. Historisk museum, Universitetet i Bergen (151 pp).

Berglund, B.E., Björck, S., Lemdahl, G., Bergsten, H., Nordberg, K. and Kolstrup, E., 1994. Late Weichselian environmental-change in Southern Sweden and Denmark. Journal of Quaternary Science 9, 127-132.

Birks, H.H., Kristensen, D.K., Dokken, T.M. and Andersson, C., 2004. Exploratory comparisons of quantitative temperature estimates over the last deglaciation in Norway and the Norwegian Sea. In: H. Drange, T. Dokken, T. Furevik, R. Gerdes and W. Berger (Eds.), The Nordic Seas: an integrated perspective oceanography, climatology, biogeochemistry, and modelling. American Geophysical Union, Washington, 341-355.

Björck, S. and Digerfeldt, G., 1991. Allerød-Younger Dryas sea level changes in southwestern Sweden and their relation to the Baltic Ice Lake development. Boreas 20, 115-133.

Blockley, S.P.E., Lowe, J.J., Walker, M.J.C., Asioli, A., Trincardi, F., Coope, G.R., Donahue, R.E. and Pollard, A.M., 2004. Bayesian analysis of radiocarbon chronologies: examples from the European Late-glacial. Journal of Quaternary Science 19, 159-175.

Bondevik, S. and Mangerud, J., 2002. A calendar age estimate of a very late Younger Dryas ice sheet maximum in western Norway. Quaternary Science Reviews 21, 1661-1676.

Bondevik, S., Mangerud, J., Dawson, S., Dawson, A. and Lohne, Ø., 2005. Evidence for three North Sea tsunamis at the Shetland Islands between 8000 and 1500 years ago. Quaternary Science Reviews 24, 1757-1775.

Bondevik, S., Mangerud, J., Birks, H.H., Gulliksen, S. and Reimer, P., submitted. Changes in North Atlantic radiocarbon reservoir ages during Allerød and Younger Dryas. Submitted to Science.

Bondevik, S., Svendsen, J.I., Johnsen, G., Mangerud, J. and Kaland, P.E., 1997a. The Storegga tsunami along the Norwegian coast, its age and runup. Boreas 26, 29-53.

Bondevik, S., Svendsen, J.I. and Mangerud, J., 1997b. Tsunami sedimentary facies deposited by the Storegga tsunami in shallow marine basins and coastal lakes, western Norway. Sedimentology 44, 1115-1131.

Bondevik, S., Svendsen, J.I. and Mangerud, J., 1998. Distinction between the Storegga tsunami and the marine transgression in coastal basins deposits of western Norway. Journal of Quaternary Science 13, 529-537.

Bronk Ramsey, C., 2005. The OxCal radiocarbon calibration software, v3.10.

Coope, G.R. and Lemdahl, G., 1995. Regional differences in the Lateglacial climate of northern Europe based on coleopteran analysis. Journal of Quaternary Science 10, 391-395.

Coope, G.R., Lemdahl, G., Lowe, J.J. and Walkling, A., 1998. Temperature gradients in northern Europe during the last glacial-Holocene transition (14-9 C-14 kyr BP) interpreted from coleopteran assemblages. Journal of Quaternary Science 13, 419-433.

Corner, G.D., 1980. Preboreal deglaciation chronology and marine limits of the Lyngen-Storfjord area, Troms, North Norway. Boreas 9, 239-249.

Davis, J.C., 1986. Statistics and data analysis in Geology. John Wiley & Sons, New York (646 pp).

de Wolf, H., 1982. Method of coding of ecological data from diatoms for computer utilization. Mededelingen Rijks Geologische Dienst 36, 95-98.

Denys, L., 1991/2. A check-list of diatoms in the Holocene deposits of the western Belgian coastal plain with a survey of their apparent ecological requirements, Professional Paper 246 (41 pp.).

Fjeldskaar, W. and Kanestrøm, R., 1980. Younger Dryas geoid-deformation caused by deglaciation in Fennoscandia. In: N.-A. Mörner (Ed.), Earth rheology, isostasy and eustasy. John Wiley & Sons, Chichester, United Kingdom, 569-574.

Fjeldskaar, W. and Kanestrøm, R., 1981. The isostatic process in Fennoscandia and inferred lithosphere and mantle rheology. In: W. Fjeldskaar (Ed.), Late-glacial movements of sea-level and crust in Fennoscandia. Dr. scient. thesis, University of Bergen, 93-145.

Flatekval, L.H., 1991. Strandforskyvning på Tau, Rogaland. Lito- og biostratigrafiske undersøkelser av tre myrbasseng ved Norwerk, University of Bergen (74+51 pp).

Fægri, K., 1940. Quartärgeologische Untersuchungen im Westlichen Norwegen. II. Zur spätquartären Geschichte Jærens. Bergen Museums Årbok, 1939-40 (201 pp).

Fægri, K., 1944. On the introduction of agriculture in western Norway. Geologiska Föreningens i Stockholm Förhandlinger 66, 449-462.

Grootes, P.M., Stuiver, M., White, J.W.C., Johnsen, S. and Jouzel, J., 1993. Comparison of Oxygen-Isotope Records from the Gisp2 and Grip Greenland Ice Cores. Nature 366, 552-554.

Grönvold, K., Òskarsson, N., Johnsen, S., Clausen, H.B., Hammer, C.U., Bond, G. and Bard, E., 1995. Ash layers from Iceland in the Greenland GRIP ice core correlated with oceanic and land sediments. Earth and Planetary Science Letters 135, 149-155.

Gudmundsson, A., 1999. Postglacial crustal doming, stresses and fracture formation with application to Norway. Tectonophysics 307, 407-419.

Haflidason, H., Sejrup, H.P., Nygard, A., Mienert, J., Bryn, P., Lien, R., Forsberg, C.F., Berg, K. and Masson, D., 2004. The Storegga Slide: architecture, geometry and slide development. Marine Geology 213, 201-234.

Hafsten, U., 1960. Pollen-analytic investigations in South Norway. In: O. Holtedahl (Ed.), Geology of Norway. Norges geologiske Undersøkelse, Oslo, 434-462.

Hendey, N.I., 1964. An introductory account of smaller algae of British coastal waters. Part V: Bacillariophyceae (Diatoms). Her majesty's stationary office, London (317 pp).

Hughen, K.A., Southen, J.R., Lehman, S.J. and Overpeck, J.T., 2000. Synchronous radiocarbon and climate shifts during the last deglaciation. Science 290, 1951-1954.

Hustedt, F., 1930. Bacillariophyta (Diatomeae). In: A. Pascher (Ed.), Die Süsswasserflora Mitteleuropas. Gustav Fischer, Jena.

Hustedt, F., 1930-66. Die Kieselalgen Deutschlands, Österreichs und der Schweiz. In: L. Rabenhorst (Ed.), Kryptogramen-Flora von Deutschland, Österreich und der Sweitz. Akademische Verlagsgesellschaft, Leipzig.

Hustedt, F., 1957. Die Diatomeenflora des Fluss-Systems der Weser im Gebiet der Hansestadt Bremen. Abhandlungen herausgegeben vom Naturwissenschaftlicher Verein zu Bremen 34, 181-440.

Håkansson, S., 1980. University of Lund radiocarbon dates XIII. Radiocarbon 22, 1045-1063.

Indrelid, S., Myhre, B., Krzywinski, K. and Sønstegaard, E., 1976. Ilandføring av olje på Sotra. Historisk Museum, Universitetet i Bergen (181 pp).

Kaland, P.E., 1984. Holocene shore displacement and shorelines in Hordaland, western Norway. Boreas 13, 203-242.

Kaland, P.E., Krzywinski, K. and Stabell, B., 1984. Radiocarbon-dating of transitions between marine and lacustrine sediments and their relations to the development of lakes. Boreas 13, 243-258.

Klitgaard-Kristensen, D., Sejrup, H.P. and Haflidason, H., 2001. The last 18 kyr fluctuations in Norwegian Sea surface conditions and implications for the

magnitude of climatic change: Evidence from the North Sea. Paleoceanography 16, 455-467.

Koç, N., Jansen, E. and Haflidason, H., 1993. Paleoceanograpic reconstructions of surface ocean conditions in the Greenland, Iceland and Norwegian Seas through the last 14 ka based on diatoms. Quaternary Science Reviews 12, 115-140.

Kolderup, C.F., 1908. Bergensfeltene og tilstötende trakter i senglacial og postglacial tid. Bergen Museums Årbok 1907:14, 266.

Krammer, K. and Lange-Bertalot, H., 1986. *Süsswasserflora von Mitteleuropa*, Band 2/1, Bacillariophyceae. 1. Teil Naviculaceae. Fischer, Stuttgart (876 pp).

Krammer, K. and Lange-Bertalot, H., 1988. *Süsswasserflora von Mitteleuropa*, Band 2/2, Bacillariophyceae. 2. Teil Epithemiaceae, Bacillariaceae, Surirellaceae. Fischer, Stuttgart (596 pp).

Krammer, K. and Lange-Bertalot, H., 1991a. *Süsswasserflora von Mitteleuropa*, Band 2/3, Bacillariophyceae. 3. Teil Centrales, Fragilariaceae, Eunotiaceae. Fischer, Stuttgart (576 pp).

Krammer, K. and Lange-Bertalot, H., 1991b. *Süsswasserflora von Mitteleuropa*, Band 2/4, Bacillariophyceae. 4. Teil Achnanthaceae, kritische Ergänzungen zu Navicula (Lineolatae) und Gomponema: Gesamtliteraturverzeichnis Teil 1-4. Fischer, Stuttgart (437 pp).

Kristiansen, I.L., Mangerud, J. and Lømo, L., 1988. Late Weichselian/early Holocene pollen- and lithostratigrahy in lakes in the Ålesund area, Western Norway. Review of Palaeobotany and Palynology 53, 185-231.

Krzywinski, K. and Stabell, B., 1978. Senglasiale undersøkelser på Sotra. Arkeo 1978:1, 27-31.

Krzywinski, K. and Stabell, B., 1984. Late Weichselian sea level changes at Sotra, Hordaland, Western Norway. Boreas 13, 159-202.

Lambeck, K., Antonioli, F., Purcell, A. and Silenzi, S., 2004. Sea-level change along the Italian coast for the past 10,000 yr. Quaternary Science Reviews 23, 1567-1598.

Lambeck, K., Yokoyama, Y. and Purcell, T., 2002. Into and out of the Last Glacial Maximum: sea-level change during Oxygen Isotope Stages 3 and 2. Quaternary Science Reviews 21, 343-360.

Larsen, E., Attig, J.W., Aa, A.R. and Sønstegaard, E., 1998. Late-glacial cirque glaciation in parts of western Norway. Journal of Quaternary Science 13, 17-27.

Lohne, Ø.S., Bondevik, S., Mangerud, J. and Schrader, H., 2004. Calendar year age estimates of Allerød - Younger Dryas sea-level oscillations at Os, western Norway. Journal of Quaternary Science 19, 443-464.

Mangerud, J., 1977. Late Weichselian marine sediments containing shells, foraminifera, and pollen, at Ågotnes, Western Norway. Norsk geologisk Tidsskrift 57, 23-54.

Mangerud, J., 1980. Ice-front variations of different parts of the Scandinavian Ice Sheet, 13 000-10 000 Years B.P. In: J.J. Lowe, J.M. Gray and J.E. Robinson (Eds.), Studies in the lateglacial of North-West Europe: including papers presented at a

symposium of the Quaternary Research Association held at University College London, January 1979. Pergamon Press, Oxford, 23-30.

Mangerud, J., 1987. The Allerød/Younger Dryas boundary. In: W.H. Berger and L. Labeyrie (Eds.), Abrupt climatic change - evidence and implications. D. Reidel, Dordrecht, 163-171.

Mangerud, J., 2004. Ice sheet limits on Norway and the Norwegian continental shelf. In: J. Ehlers and P. Gibbard (Eds.), Quaternary Glaciations - Extent and Chronology. Vol 1. Europe. Elsevier, Amsterdam, 271-294.

Mangerud, J. and Gulliksen, S., 1975. Apparent radiocarbon ages of recent marine shells from Norway, Spitsbergen and Arctic Canada. Quaternary Research 5(2), 263-273.

Mangerud, J., Lie, S.E., Furnes, H., Kristiansen, I.L. and Lømo, L., 1984. A Younger Dryas Ash Bed in Western Norway, and its possible correlations with tephra in cores from the Norwegian Sea and the North Atlantic. Quaternary Research 21, 85-104.

Olesen, O., Blikra, L.H., Braathen, A., Dehls, J.F., Olsen, L., Rise, L., Roberts, D., Riis, F., Faleide, J.I. and Anda, E., 2004. Neotectonic deformation in Norway and its implications: a review. Norwegian Journal of Geology 84, 3-34.

Paus, A., 1989. Late Weichselian vegetation, climate, and floral migration at Liastemmen, North-Rogaland, south-western Norway. Journal of Quaternary Science 4, 223-242.

Peltier, W.R., 2004. Global glacial isostasy and the surface of the ice-age earth: The ice-5G (VM2) model and GRACE. Annual Review of Earth and Planetary Sciences 32, 111-149.

Reimer, P.J., Baillie, M.G.L., Bard, E., Bayliss, A., Beck, J.W., Bertrand, C.J.H., Blackwell, P.G., Buck, C.E., Burr, G.S., Cutler, K.B., Damon, P.E., Edwards, R.L., Fairbanks, R.G., Friedrich, M., Guilderson, T.P., Hogg, A.G., Hughen, K.A., Kromer, B., McCormac, G., Manning, S., Ramsey, C.B., Reimer, R.W., Remmele, S., Southon, J.R., Stuiver, M., Talamo, S., Taylor, F.W., van der Plicht, J. and Weyhenmeyer, C.E., 2004. IntCal04 Terrestrial Radiocarbon Age Calibration, 0-26 Cal Kyr BP. Radiocarbon 46, 1029-1058.

Shepard, F.P., 1963. Thirthy-five thousand years of sea-level. In: T. Clements (Ed.), Essays in Marine Geology in Honor of K.O. Emery. Southern California Press, Los Angeles, 1-10.

Stabell, B., 1985. The development and succession of taxa within the diatom genus *Fragilaria* Lyngbye as a response to basin isolation from the sea. Boreas 14, 273-286.

Stabell, B. and Krzywinski, K., 1978. Strandforskyvningsundersøkelsen. In: B. Myhre (Ed.), Statfjord Transportation System Project. Ilandføring av olje på Sotra. De arkeologiske undersøkelser 1978. Vindenes. Historisk museum, Universitetet i Bergen, 93-132.

Stabell, B. and Krzywinski, K., 1979. Havnivåendringer på Sotra, Hordaland. Arkeo 1, 12-15.

Svendsen, J.I. and Mangerud, J., 1987. Late Weichselian and Holocene sea-level history for a cross-section of western Norway. Journal of Quaternary Science 2, 113-132.

Thomsen, H., 1982. Late Weichselian shore-level displacement on Nord-Jæren, south-west Norway. Geologiska Föreningens i Stockholm Förhandlinger 103, 447-468.

Tidevannstabeller, 1998. Tidevannstabeller for den norske kyst med Svalbard samt Dover, England 1999. Statens kartverk, sjøkartverket.

Walker, M.J.C., Coope, G.R., Sheldrick, C., Turney, C.S.M., Lowe, J.J., Blockley, S.P.E. and Harkness, D.D., 2003. Devensian Lateglacial environmental changes in Britain: a multi-proxy environmental record from Llanilid, South Wales, UK. Quaternary Science Reviews 22, 475-520.

Witkowski, A., Lange-Bertalot, H. and Metzeltin, B., 2000. Diatom flora of marine coasts I. ARG Gantner Verlag K.G.

Aarseth, I. and Mangerud, J., 1974. Younger Dryas end moraines between Hardangerfjorden and Sognefjorden, Western Norway. Boreas 3, 3-22.

Table 1 Diatom salinity groups after Hustedt (1957).

Halobion group	Salinity tolerance
Polyhalobous	Marine water taxa (>30‰ salinity)
Mesohalobous	Brackish water taxa (30-0.2‰ salinity)
Oligohalobous halophilous	Taxa that can live in both brackish and fresh water, optimum in brackish water
Oligohalobous indifferent	Taxa that can live in both brackish and fresh water, optimum in fresh water
Halophobous	Fresh water taxa (<0.2‰salinity)

Table 2 Radiocarbon dates from the basins investigated in the present study.

Locality	Core	Depth (cm)	Terrestrial plant material dated	Submitted sample weight (mg)	Laboratory number	^{14}C age (yr BP)
Gardatjønn	505-121	1144.5 - 1147.5	Leaf fragments, wood, moss stems	3.54	Poz-6368	9520 ± 50
Gardatjønn	505-121	1150.5 - 1152.5	Leaf fragments, twig, wood	4.48	Poz-6369	9780 ± 50
Gardatjønn	505-121	1153.5 - 1155.5	Leaves (3), leaf fragments, *Racomitrium*	6.66	Poz-6370	9890 ± 50
Gardatjønn	505-121	1155.5 - 1156.5	Leaf fragments (*S. herbacea*)	5.65	Poz-6371	10 080 ± 50
Gardatjønn	505-27	1158.5 - 1159.5	*S. herbacea* leaves (3), leaf fragments	6.08	Poz-5130	10 040 ± 50
Gardatjønn	505-121	1159.5 - 1160.5	*S. herbacea* and *S. polaris* leaves, *Racomitrium*	11.75	Poz-5129	10 050 ± 50
Gardatjønn	505-27	1160.5 - 1161.5	*S. herbacea* leaves, leaf fragments	5.12	Poz-5185	9980 ± 50
Gardatjønn	505-27	1161.5 - 1162.5	*S. herbacea* leaves	7.82	Poz-5133	10 090 ± 60
Gardatjønn	505-27	1167.5 - 1168.5	*S. herbacea* leaves (4), *Racomitrium*, leaf fragments	4.88	Poz-5134	10 060 ± 60
Gardatjønn	505-27	1168.5 - 1169.5	*S. herbacea* leaves (3), *Racomitrium*, leaf fragments	5.17	Poz-5135	10 170 ± 60
Gardatjønn	505-27	1169.5 - 1170.5	Twig, leaf fragments	3.90	Poz-6372	10 090 ± 50
Gardatjønn	505-27	1171.5 - 1172.5	Twigs (2), leaf fragments	5.10	Poz-5136	10 270 ± 50
Gardatjønn	505-121	1186.5 - 1187.5	Leaves and leaf fragment, *Racomitrium*	9.15	Poz-5184	10 940 ± 60
Gardatjønn	505-121	1187.5 - 1188.5	*S. herbacea* and *S. polaris* leaves, *Racomitrium*	7.49	Poz-5131	10 910 ± 60
Gardatjønn	505-121	1199.5 - 1200.5	Leaf fragments	5.30	Poz-5132	12 130 ± 60
Gardatjønn	505-27	1201.5 - 1203.5	Leaf fragments	4.24	Poz-5137	11 720 ± 60
Hamravatn	505-19	1278 - 1280	S. herbacea, *Racomitrium*	27.16	Poz-4811	10 370 ± 50
Hamravatn	505-19	1285 - 1287	*S. herbacea*, *Racomitrium*, twig	5.51	Poz-4812	10 820 ± 60
Hamravatn	505-19	1290 - 1292	Bud scales (2), *Racomitrium*, twig	8.07	Poz-4813	11 080 ± 50
Hamravatn	505-19	1292 - 1294	*S. polaris* , *Racomitrium*	22.64	Poz-4814	11 070 ± 60
Hamravatn	505-19	1294 - 1296	*S. polaris*, *Polytricum*, *Racomitrium*	11.52	Poz-4815	11 090 ± 50
Hamravatn	505-19	1312 - 1314	*Racomitrium*, *Polytricum*, twig	3.86	Poz-4817	12 090 ± 60
Hamravatn	505-19	1348 - 1350	Leaf fragments, mosses	2.56	Poz-4818	12 270 ± 70
Sekkingstadtjønn	505-102	1252.5 - 1253.5	*Dryas* and *S. herbacea* leaves, *Racomitrium*	11.72	Poz-4908	10 700 ± 60
Sekkingstadtjønn	505-102	1292.5 - 1293.5	*Racomitrium*, bud scale, leaf fragments	5.71	Poz-5095	11 320 ± 70
Sekkingstadtjønn	505-102	1293.5 - 1294.5	*Racomitrium*, *Polytricum*, leaf fragments	16.11	Poz-5096	11 440 ± 70
Sekkingstadtjønn	505-102	1294.5 - 1295.5	*S. herbacea* leaves, twigs, *Racomitrium*, *Polytricum*	6.13	Poz-4909	11 310 ± 60
Sekkingstadtjønn	505-102	1295.5 - 1296.5	*Racomitrium*, fragments of *S. herbacea* leaves	11.80	Poz-4910	11 310 ± 60
Sekkingstadtjønn	505-102	1296.5 - 1297.5	*S. herbacea* leaves (4), *Racomitrium*, leaf fragments	20.30	Poz-4911	11 450 ± 60
Sekkingstadtjønn	505-102	1297.5 - 1298.5	*Racomitrium*, *S. herbacea* leaves, leaf fragments	14.31	Poz-4912	11 430 ± 60
Sekkingstadtjønn	505-102	1298.5 - 1299.5	*Racomitrium*, *Polytricum*, leaf fragments	11.39	Poz-4819	11 310 ± 60
Sekkingstadtjønn	505-102	1299.5 - 1300.5	*Racomitrium*, *S. herbacea* leaf, leaf fragments	16.61	Poz-4914	11 470 ± 60
Sekkingstadtjønn	505-102	1300.5 - 1301.5	*Racomitrium*, leaf fragments	12.52	Poz-4915	11 560 ± 60
Sekkingstadtjønn	505-102	1301.5 - 1302.5	*Racomitrium*, *Polytricum*, leaf fragments	8.83	Poz-4821	11 720 ± 60
Sekkingstadtjønn	505-102	1302.5 - 1303.5	*Racomitrium*, *Polytricum*, leaf stem	4.87	Poz-4922	11 830 ± 60
Sekkingstadtjønn	505-102	1319.5 - 1321.5	*Racomitrium*, leaf fragments	7.13	Poz-4823	12 040 ± 60

Table 3 Calendar year estimates for events dated in the present study by series of TPM ^{14}C dates, listed in chronological order. The calibration and the Bayesian probability calculations are performed using the OxCal v3.10 software (Bronk Ramsey, 2005) with the INTCAL04 calibration curve (Reimer et al., 2004). The posterior probability distributions are calculated using the *Sequence* function in OxCal.

Event	**Depth (cm)**	**^{14}C age (yr BP)**	**Calibrated single date –1σ /2σ (cal yr BP)**	**OxCal - Posterior intervals 1σ/2σ (cal yr BP)**	**OxCal – Weighted average of posterior distribution (cal yr BP)**
Hamravatn: Isolation	1313	12 090 ± 60	14 020 – 13 860 14 090 – 13 790	14 000 – 13 850 14 070 – 13 790	13 920
Sekkingstadtjønn: Isolation	1303	11 830 ± 60	13 780 – 13 630 13 820 – 13 490	13 720 – 13 470 13 760 – 13 450	13 610
Sekkingstadtjønn: Ingression	1291	-	-	13 200 – 13 060 13 240 – 12 930	13 110
Hamravatn: Ingression	1290	11 080 ± 50	13 060 – 12 930 13 100 – 12 900	12 980 – 12 910 13 030 – 12 880	12 950
Gardatjønn: Ingression	1169	10 170 ± 60	12 000 – 11 720 12 090 – 11 500	11 830 – 11 700 11 940 – 11 640	11 780
Gardatjønn: Isolation	1161	9980 ± 50	11 610 – 11 290 11 710 – 11 250	11 620 – 11 470 11 700 – 11 420	11 560

Table 4 Age calibrated and tilt corrected sea-level index points from other studies at Sotra, listed chronologically. The corrected elevation is calculated based on a baseline trough Gardatjønn with direction 351±4°. Tilt gradients are from the present study and Kaland (1984). The dates are of bulk organic matter, except for Kvaltjern, performed on terrestrial plant material. Calibration performed with the OxCal program (Bronk Ramsey, 2005) and the INTCAL04 dataset (Reimer et al., 2004). ([1]) – probably affected by the Storegga tsunami (Bondevik et al., 1997a) and omitted in the sea-level curve.

Locality (no. in Fig. 1 and 7)	Geo-ref (lat, long)	Present elevation (m a.s.l.)	Tilt corr. elevation (m a.s.l.)	Distance baseline (km)	Tilt gradient (m km^{-1})	Lab. number	^{14}C age (yr BP)	Calibrated age (1σ – cal yr BP)	Calibrated age (2σ – cal yr BP)	Event	Reference
Kvernavatn (1)	60°22.6'N, 05°02.9'E	38.2 ± 0.5	38.9 ± 1.4	0.57 ± 0.65	1.3	No marine sediments at base. Upper limit of the sea level at deglaciation					Krzywinski & Stabell (1984)
Klæsvatn (2)	60°11.8'N, 05°03.5'E	30.5 ± 0.5	34.9 ± 1.5	3.37 ± 0.74	1.3	T-2896A	12 080 ± 210	15 150 – 13 750	15 450-13 450	Isolation	Krzywinski & Stabell (1984)
Storevatn (3)	60°10.9'N, 05°03.2'E	22.6 ± 0.5	26.1 ± 1.4	2.71 ± 0.7	1.3	No lacustrine Allerød sediments. Lower limit of the Allerød regression minimum					Krzywinski & Stabell (1984)
Klæsvatn (2)	60°11.8'N, 05°03.5'E	30.5 ± 0.5	34.9 ± 1.5	3.37 ± 0.74	1.3	T-2895A	11 320 ± 120	13 440-13 150	13 800-13 000	Ingression	Krzywinski & Stabell (1984)
Kvernavatn (1)	60°22.6'N, 05°02.9'E	38.2 ± 0.5	38.9 ± 1.4	0.57 ± 0.65	1.3	Lu-1552	10 870 ± 195	13 120-12 670	13 150-12 630	Ingression	Krzywinski & Stabell (1984)
Førekleivsvatn (4)	60°17.7'N, 05°04.6'E	40.5 ± 0.5	41.3 ± 0.5	0.59 ± 0.03	1.3	No marine sediments. Upper limit of the YD transgression.					Krzywinski & Stabell (1984)
Storetjønn (5)	60°12.1'N, 05°04.1'E	38.2 ± 0.5	39.3 ± 1.4	2.71 ± 0.7	1.3	T-2636	10 180 ± 120	12 100-11 500	12 450-11 250	Isolation	Krzywinski & Stabell (1984)
Kvernavatn (1)	60°22.6'N, 05°02.9'E	35.8 ± 0.5	38.9 ± 1.4	0.57 ± 0.65	1.3	T-2892A	9980 ± 180	11 850-11 200	12 250-10 750	Isolation	Krzywinski & Stabell (1984)
Krokavatn (6)	60°23.1'N, 05°00.5'E	34.7 ± 0.5	38.1 ± 1.5	2.65 ± 0.75	1.3	T-2889A	10 150 ± 180	12 100-11 350	12 650-11 150	Isolation	Krzywinski & Stabell (1984)
Tresstjønn (7)	60°23.2'N, 04°59.7'E	32.5 ± 0.5	36.8 ± 1.5	3.33 ± 0.76	1.3	Lu-1529A	10 260 ± 100	12 350-11 750	12 650-11 450	Isolation	Krzywinski & Stabell (1984)
Klæsvatn (2)	60°11.8'N, 05°03.5'E	30.5 ± 0.5	34.9 ± 1.5	3.37 ± 0.74	1.3	T-2885A	9970 ± 130	11 700-11 240	12 000-11 150	Isolation	Krzywinski & Stabell (1984)
Hamravatn	60°12.4'N, 05°05.2'E	29.1 ± 0.5	31.3 ± 1.4	1.66 ± 0.67	1.3	T-2632	10 130 ± 120	12 000-11 400	12 250-11 250	Isolation	Krzywinski & Stabell (1984)
Sekkingstadtjønn	60°21'.0N, 04°59.6'E	24.3 ± 0.5	29.6 ± 1.1	4.04 ± 0.49	1.3	Lu-1503A	9920 ± 90	11 610-11 220	11 750-11 150	Isolation	Krzywinski & Stabell (1984)
Storevatn (3)	60°10.9'N, 05°03.4'E	22.6 ± 0.5	24.5 ± 0.9	3.74 ± 0.85	0.5	T-2888A	9470 ± 110	11 070-10 570	11 200-10 400	Isolation	Krzywinski & Stabell (1984)
Kvaltjern (8)	60°25.4'N, 04°58.8'E	17.8 ± 0.5	19.5 ± 1	3.49 ± 1.05	0.5	TUa-3242	9315 ± 70	10 650-10 410	10 700-10 280	Isolation	Bondevik et al. (submitted)
Kvaltjern (8)	60°25.4'N, 04°58.8'E	17.8 ± 0.5	19.5 ± 1	3.49 ± 1.05	0.5	TUa-3242	9315 ± 70	Wiggle matched age: 10 975		Isolation	Bondevik et al. (submitted)
Lommatjønn (9)	60°14.9'N, 05°02.2'E	11.2 ± 0.5	13 ± 0.7	3.56 ± 0.33	0.5	Lu-1353A	9290 ± 95	10 590-10 290	10 710-10 240	Isolation	Stabell & Krzywinski (1978)
Einerhaugtjønn (10)	60°21.2'N, 04°59.3'E	9.2 ± 0.5	11.4 ± 0.8	4.31 ± 0.51	0.5	Lu-1498A	9460 ± 90	11 070-10 570	11 150-10 400	Isolation	Stabell & Krzywinski (1978)
Storavatn (11)	60°14.2'N, 05°10.8'E	13.0 ± 1.0	11 ± 1.3	-4.01 ± 0.51	0.5	Lu-1581A	9420 ± 85	10 770-10 510	11 100-10 400	Isolation	Håkansson (1980)
Kaldavatn (12)	60°15.8'N, 04°58.7'E	7.6 ± 0.5	10.8 ± 0.6	6.43 ± 0.17	0.5	Lu-1361A	9340 ± 90	10 690-10 420	10 800-10 250	Isolation	Stabell & Krzywinski (1978)
Skittjønn (13)	60°14.4'N, 05°02.0'E	8.5 ± 0.5	10.3 ± 0.7	3.94 ± 0.38	0.5	T-2886A	9190 ± 140	10 550-10 220	10 750-9900	Isolation	Stabell & Krzywinski (1979)
Klokkarvatnet (14)	60°14.9'N, 05°01.8'E	6.9 ± 0.5	8.7 ± 0.6	3.95 ± 0.32	0.5	Lu-1357A	9150 ± 100	10 490-10 220	10 650-10 150	Isolation	Stabell & Krzywinski (1978)

Continues

Table 4. Continued

Locality (no. in Fig. 1 and 7)	Geo-ref (lat, long)	Present elevation (m a.s.l.)	Tilt corr. elevation (m a.s.l.)	Distance baseline (km)	Tilt gradient (m km^{-1})	Lab. number	^{14}C age (yr BP)	Calibrated age (1σ – cal yr BP)	Calibrated age (2σ – cal yr BP)	Event	Reference
Trollabotn (15)	60°26.6'N, 04°59.9'E	4.8 ± 0.5	5.7 ± 1	2.08 ± 1.19	0.5	T-2891A	9020 ± 100	10 270-9920	10 500-9750	Isolation	Kaland et al. (1984)
Trollabotn (15)[1]	60°26.6'N, 04°59.9'E	4.8 ± 0.5	5.5 ± 0.9	2.08 ± 1.19	0.4	T-2890A	8260 ± 110	9410-9090	9490-9000	Ingression[1]	Kaland et al. (1984)
Kaldavatn (12)	60°15.8'N, 04°58.7'E	7.6 ± 0.5	9.9 ± 0.6	6.43 ± 0.17	0.4	Lu-1360A	8060 ± 85	9090-8770	9250-8600	Ingression	Stabell & Krzywinski (1978)
Skittjønn (13)	60°14.4'N, 05°02.0'E	8.5 ± 0.5	9.9 ± 0.6	3.94 ± 0.38	0.4	T-2887A	7950 ± 110	8980-8640	9150-8500	Ingression	Stabell & Krzywinski (1979)
Einerhaugtjønn (10)[1]	60°21.2'N, 04°59.3'E	9.2 ± 0.5	10.5 ± 0.7	4.31 ± 0.51	0.3	Lu-1497A	7720 ± 80	8580-8420	8650-8370	Ingression[1]	Stabell & Krzywinski (1978)
Lommatjønn (9)	60°14.9'N, 05°02.2'E	13.0 ± 1.0	11.8 ± 1.2	-4.01 ± 0.51	0.3	Lu-1354A	7400 ± 100	8280-8020	8330-8000	Ingression	Kaland et al. (1984)
Storavatn (11)[1]	60°14.2'N, 05°10.8'E	11.2 ± 0.5	12.3 ± 0.6	3.56 ± 0.33	0.3	Lu-1580A	7330 ± 75	8350-8060	8390-8010	Tapes max [1]	Stabell & Krzywinski (1979)
Torkevikstjønn (16)	60°23.3'N, 04°58.5'E	11.8 ± 0.5	12.7 ± 0.7	4.4 ± 0.79	0.2	Lu-1553A	6050 ± 70	7000-6790	7160-6740	Tapes max	Stabell & Krzywinski (1978)
Lommatjønn (9)	60°14.9'N, 05°02.2'E	11.2 ± 0.5	11.7 ± 0.6	3.56 ± 0.33	0.2	Lu-1355A	5490 ± 65	6400-6210	6440-6120	Isolation	Kaland et al. (1984)
Einerhaugtjønn (10)	60°21.2'N, 04°59.3'E	9.2 ± 0.5	9.6 ± 0.6	4.31 ± 0.51	0.1	Lu-1496A	4880 ± 65	5710-5480	5750-5460	Isolation	Stabell & Krzywinski (1978)
Skittjønn (13)	60°14.4'N, 05°02.0'E	8.5 ± 0.5	8.9 ± 0.5	3.94 ± 0.38	0.1	T-2884A	4410 ± 50	5220-4870	5280-4850	Isolation	Stabell & Krzywinski (1979)
Midtjønn (17)	60°14.6'N, 05°0.02'E	7.9 ± 0.5	8.3 ± 0.5	3.81 ± 0.36	0.1	Lu-1358A	4260 ± 60	4950-4650	4980-4610	Isolation	Stabell & Krzywinski (1978)
Kaldavatn (12)	60°15.8'N, 04°58.7'E	7.6 ± 0.5	8.2 ± 0.5	6.43 ± 0.17	0.1	Lu-1359A	4340 ± 60	4980-4840	5280-4820	Isolation	Stabell & Krzywinski (1978)
Klokkarvatnet (14)	60°14.9'N, 05°01.8'E	6.9 ± 0.5	7.3 ± 0.5	3.95 ± 0.32	0.1	Lu-1356A	3990 ± 60	4570-4300	4800-4200	Isolation	Stabell & Krzywinski (1978)
Vestretjønn (18)	60°14.4'N, 05°10.0'E	7.3 ± 0.5	7 ± 0.5	-3.36 ± 0.47	0.1	Lu-1583A	3600 ± 55	3980-3830	4090-3720	Isolation	Håkansson (1980)
Bakketjønn (19)	60°22.7'N, 04°59.0'E	5.3 ± 0.5	5.5 ± 0.5	4.11 ± 0.71	0.1	Lu-1495A	2790 ± 55	2960-2790	3040-2760	Isolation	Stabell & Krzywinski (1978)
Austretjønn (20)	60°14.5'N, 05°10.2'E	5.7 ± 0.5	5.5 ± 0.5	-3.57 ± 0.46	0.1	Lu-1582A	2860 ± 55	3070-2880	3170-2840	Isolation	Håkansson (1980)
Skrubbisvatn (21)	60°15.7'N, 04°58.4'E	3.5 ± 0.5	3.8 ± 0.5	6.76 ± 0.19	0.1	Lu-1528A	2490 ± 55	2720-2470	2740-2360	Isolation	Stabell & Krzywinski (1978)
Angeltveitvatnet (22)	60°24.4'N, 04°59.3'E	3.6 ± 0.5	3.8 ± 0.5	3.29 ± 0.92	0.1	Lu-1527A	2240 ± 55	2340-2150	2350-2130	Isolation	Stabell & Krzywinski (1978)

([1]) – probably affected by the Storegga tsunami (Bondevik et al., 1997a) and omitted in the sea-level curve.

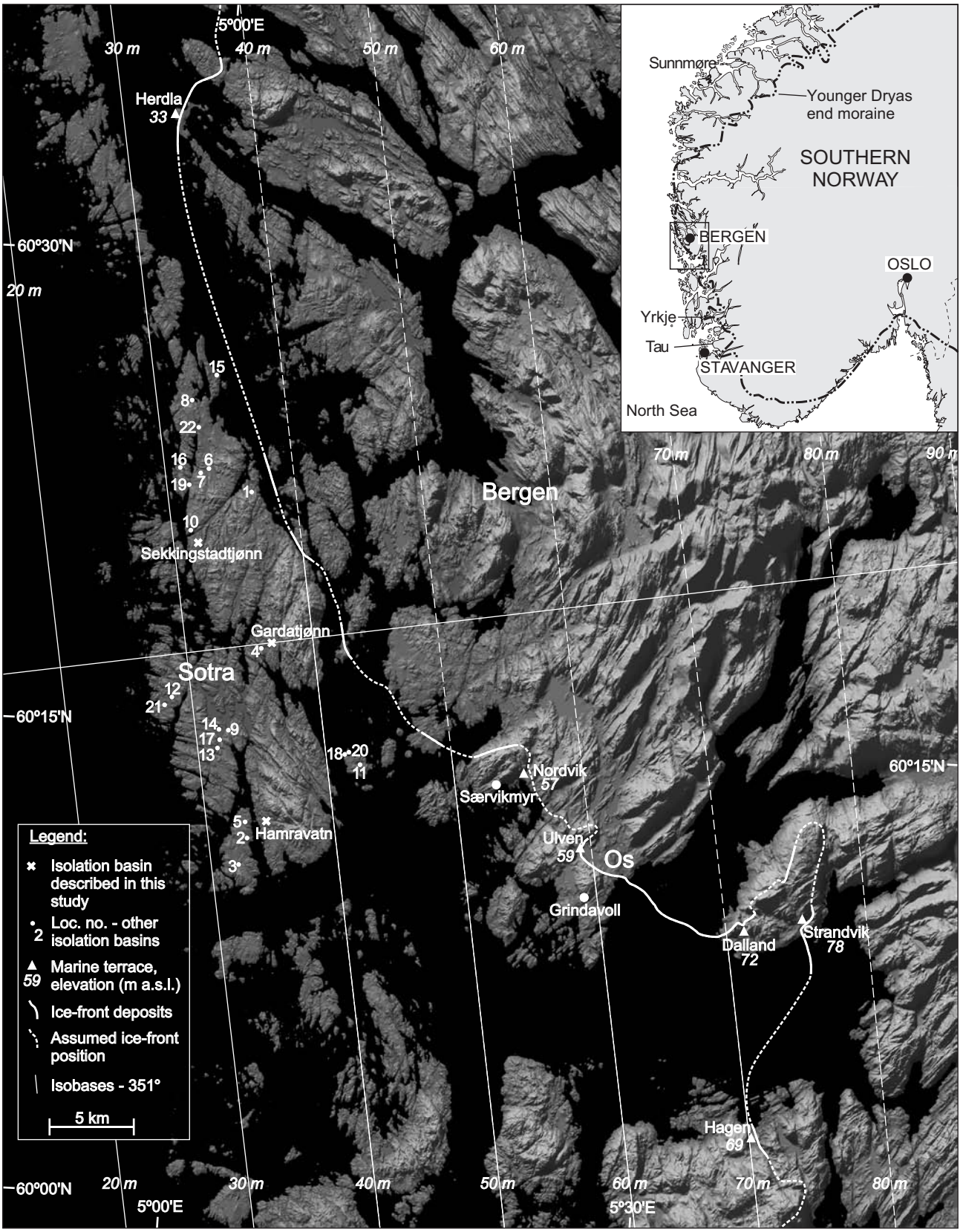

Fig. 1. Map of the studied sites in Hordaland, western Norway. The most discussed localities are indicated with names and symbols. Other localities are numbered according to Table 4. Elevations of marine terraces are adjusted to mean sea level (see text). YD isobases (stippled inside the former ice sheet) with a direction 351° are shown for every 10 m, indicating the marine limits with a late YD age (Lohne et al., 2004). The projection plane for an equidistant shoreline diagram (Fig. 11) is shown perpendicular to the isobase direction. The indicated ice front position is the Herdla Moraines (Aarseth and Mangerud, 1974) showing the maximum extension of the YD ice sheet with a late YD age (Bondevik and Mangerud, 2002). The YD ice sheet margin in southern Norway (Mangerud, 2004) is indicated on the inset map.

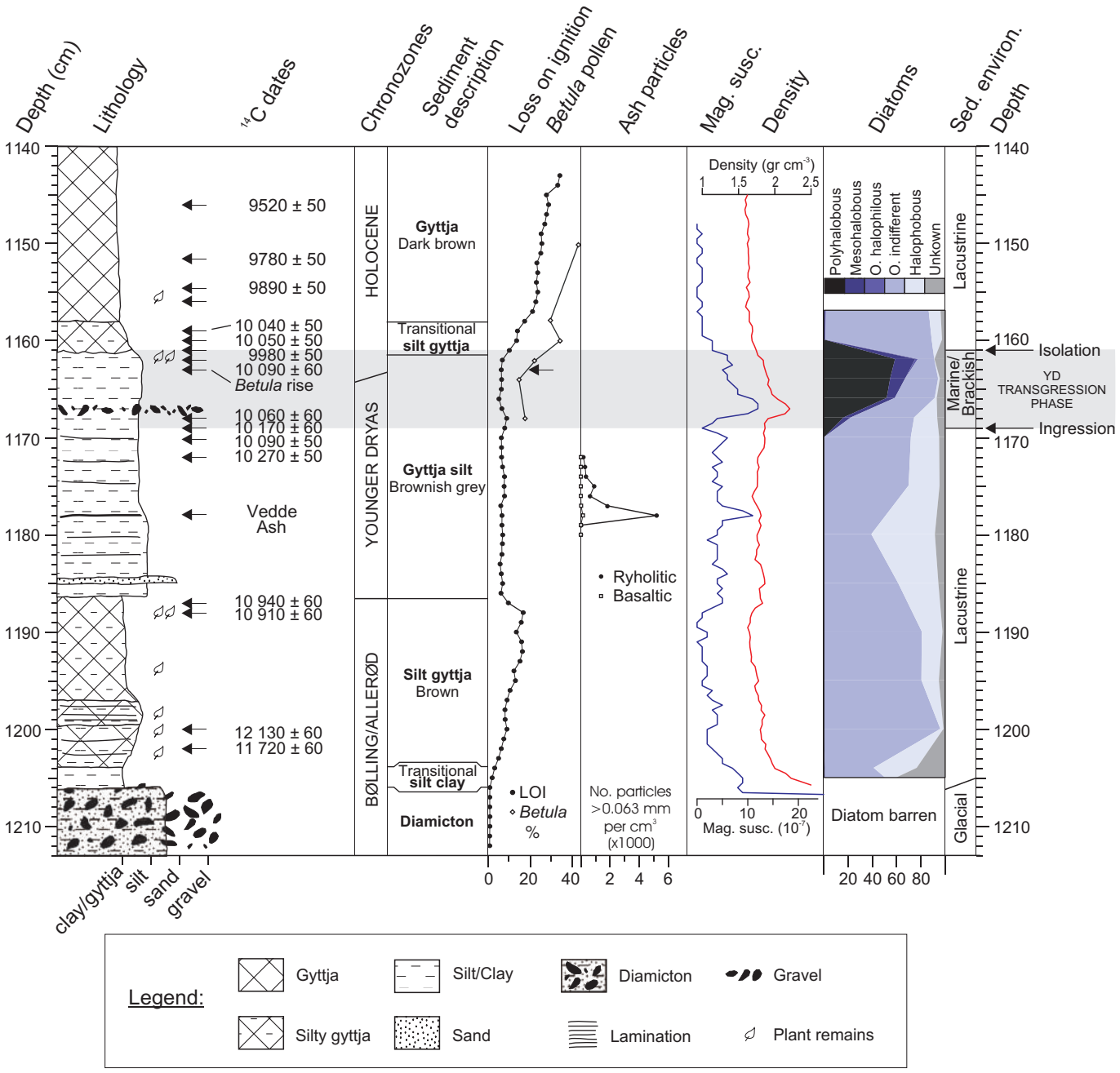

Fig. 2. The stratigraphy of core 505-27, obtained from the small lake Gardatjønn at Sotra (Fig. 1). The grey shaded area highlights a short interval of marine/brackish sediments. Detailed diatom and pollen diagrams are shown in Appendix A and B, respectively.

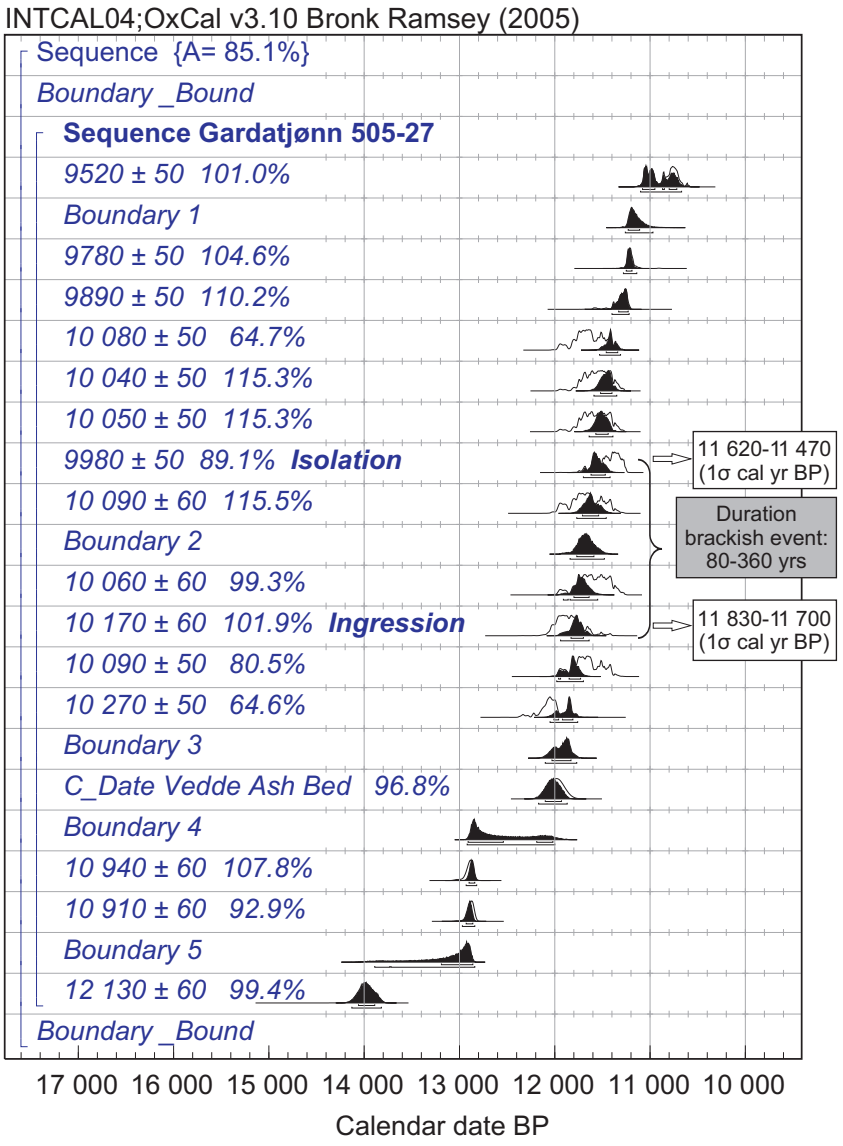

Fig. 3. Probability distributions for the ^{14}C dates from Gardatjønn calibrated in Oxcal (Bronk Ramsey, 2005) using the INTCAL04 data-set (Reimer et al., 2004). The Vedde Ash Bed is used as a calendar year date of 11 980 ± 80 cal yr BP (Grönvold et al., 1995). The prior unconstrained probability distributions are shown as clear curves. The posterior probably distributions shown as filled black curves, are constrained by Bayesian probability approach with the assumption that age increase with depth. The age intervals for the ingression and isolation contacts and the time span of the brackish phase are calendar year age estimates (1 BP) from the posterior probability distribution. The lowermost date in the core is obviously too young and was omitted in the Bayesian analysis (Fig. 2).

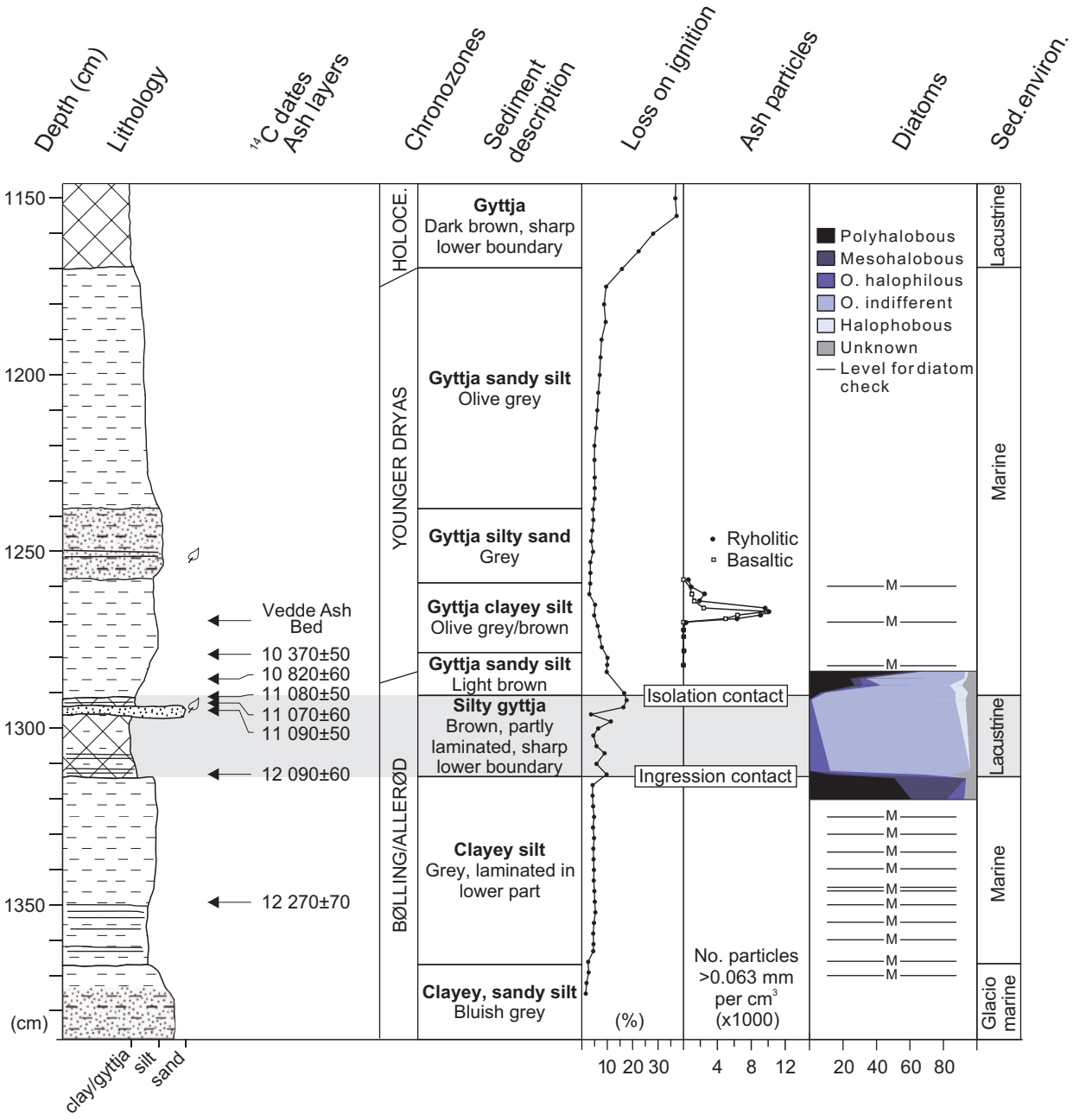

Fig. 4. The stratigraphy of the core 505-19 from the small lake Hamravatn at Sotra (Fig. 1). Highlighted in grey shade is an interval of the lacustrine sediment showing that the basin was above the sea level during the Allerød. Detailed diatom diagram is shown in Appendix C. See Fig. 2 for legend.

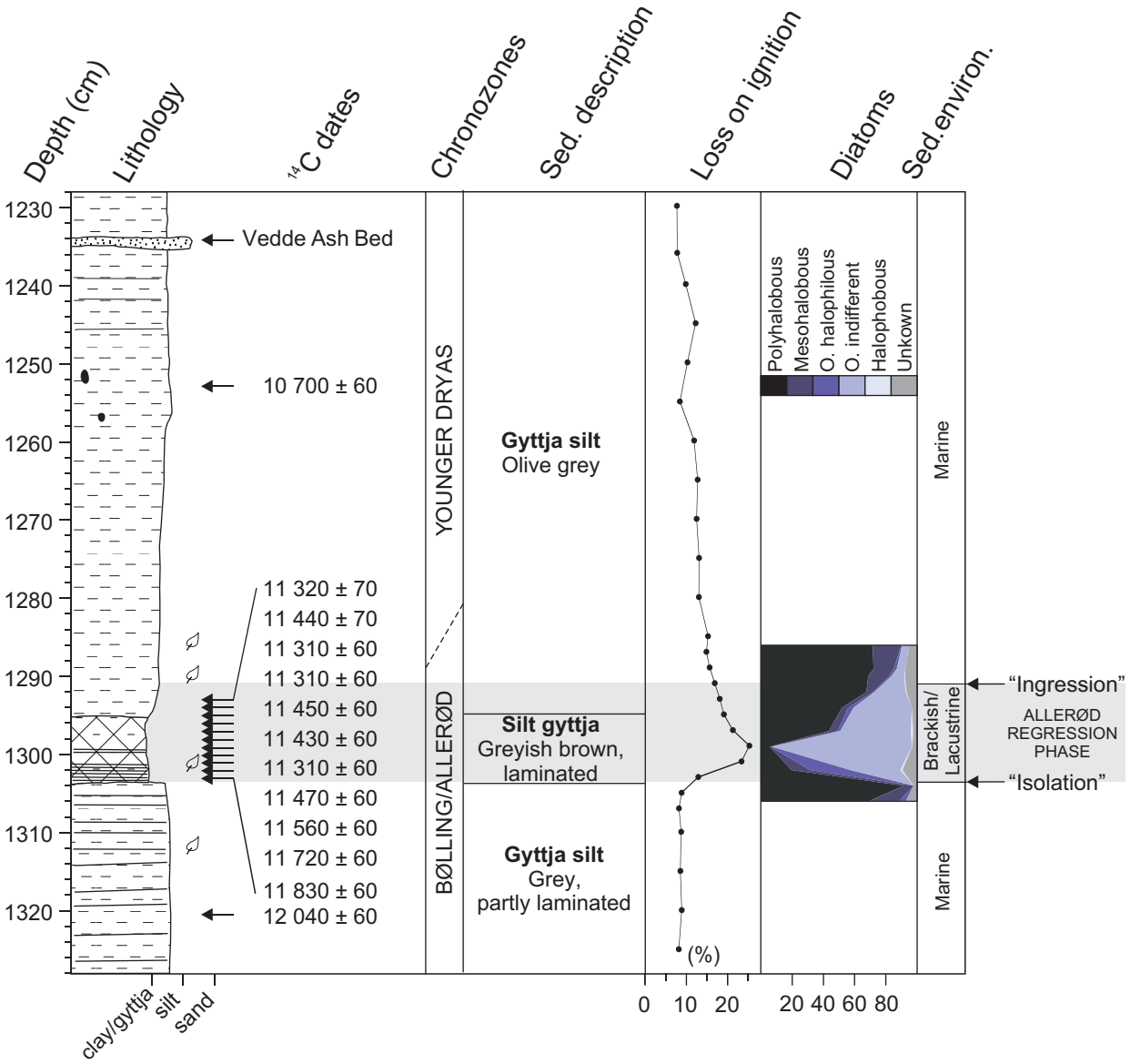

Fig. 5. The stratigraphy of core 505-102, obtained from Sekkingstadtjønn at Sotra (Fig. 1). Indicated in grey shading is an interval of brackish/lacustrine sediment, showing the sea-level lowstand (regression minimum) during the Allerød. Detailed diatom diagram is shown in Appendix D. See Fig. 2 for legend.

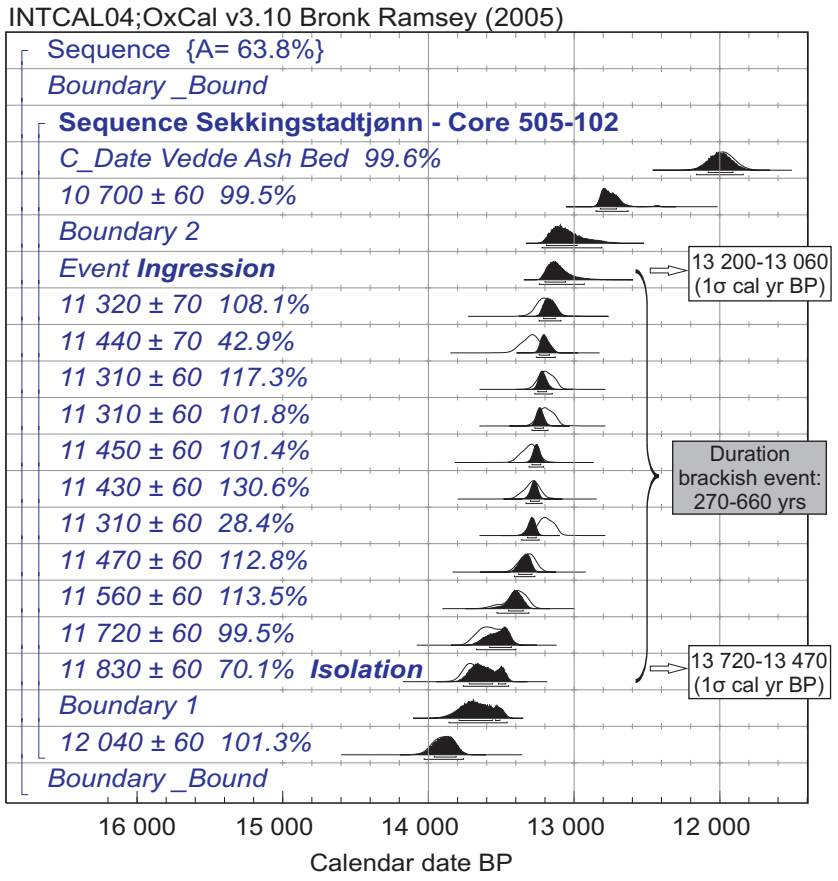

Fig. 6. Estimates of calendar year ages of the dates and events in Sekkingstadtjønn sequence employed by a Bayesian probably approach. The VeddeAsh Bed are used as a calendar year date at 11 980 ± 80 cal yr BP (Grönvold et al., 1995). Prior unconstrained probability distributions (clear) and posterior probably distributions (black) (constrained by the assumption that age should increase with depth) are shown. The age intervals for the ingression and isolation contacts and the time span of the brackish phase are calendar year age estimates (1 BP) from the posterior probability distribution.

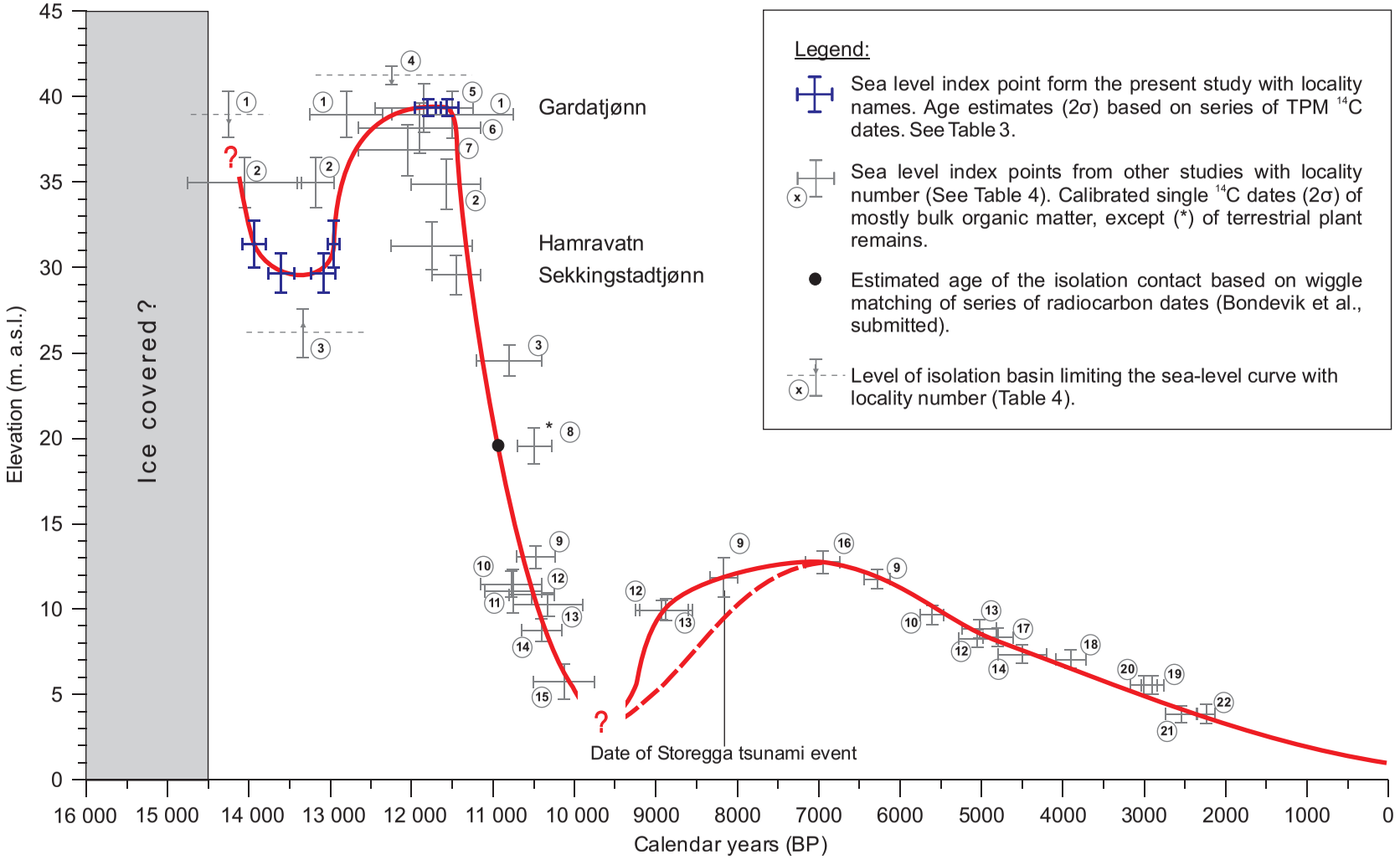

Fig. 7. Relative sea-level curve of Sotra based on isolation basin covering the last 14 500 cal years. The curve is constructed along a baseline (351±4°) through Gardatjønn (Fig. 1). The age intervals are plotted 2 level, and the height includes uncertainties from both the determination of the present basin elevation and the projection of the localities within ±4° off the baseline. Note that the tilt gradients vary trough time and the index points are adjusted individually in respect of age (Table 4).

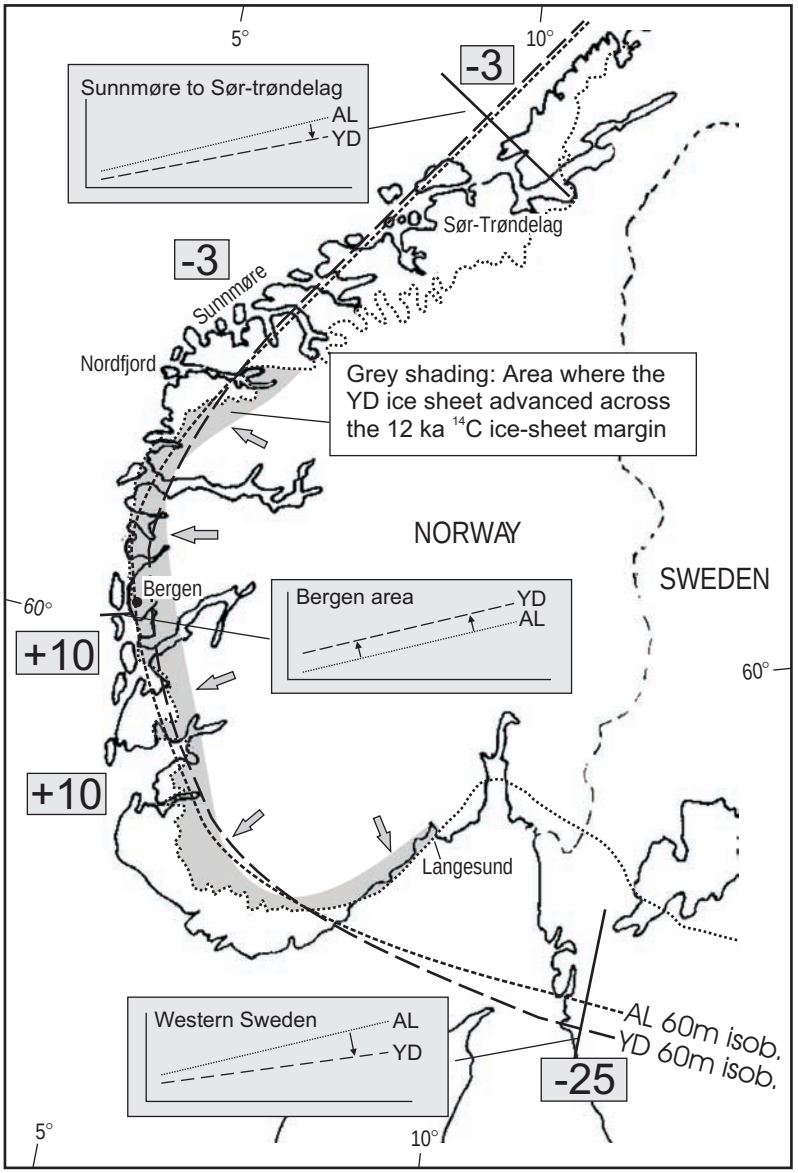

Fig. 8. Map indicating the geographical extension of the YD transgression. The relative sea-level change from late Allerød to late YD are shown as numbers in boxes, "-" for emergence and "+" for transgression. Three simplified shoreline diagrams are shown with the projection planes for each indicated by thick lines (based on Svendsen and Mangerud (1987) for Sunnmøre-Sør-Trøndelag, and Björck and Digerfeldt (1991) for SW Sweden). Note that the Allerød and YD isobases (here shown with the 60m YD isobase) crosses north and south of western Norway as a result of the YD shoreline being higher than the Allerød line along the western coast of Norway. The dotted line indicates the maximum extension of YD ice sheet. Large arrows and grey shading indicate the area where a major ice sheet readvance during the YD, which advanced beyond the 12ka ^{14}C BP ice sheet margin (Mangerud, 2004).

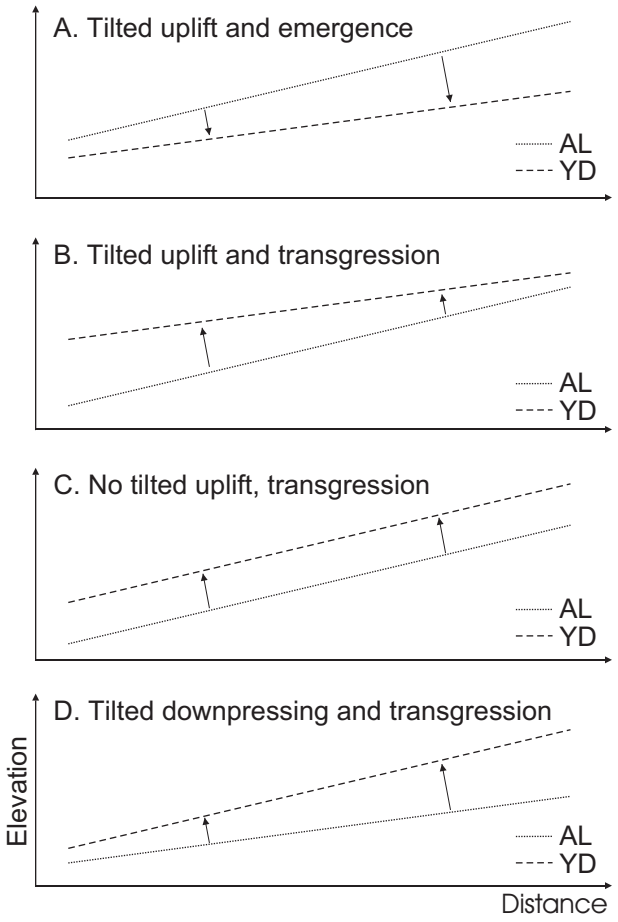

Fig. 9. Theoretical shoreline diagrams showing the tilt of the Allerød and YD shorelines for different tilted isostatic movement. Arrows show the relative sea-level change. A. The upper panel represents a typical diagram from a newly deglaciated area with tilted uplift and emergence. B. Diagram showing tilted uplift as in A, but with eustatic sea-level rise (transgression). C. In this case a transgression without any tilting. D. The lowest panel shows a case where glacio isostatic loading gave tilting in opposite direction compared to Aand B, and a transgression with or without a eustatic sea-level rise.

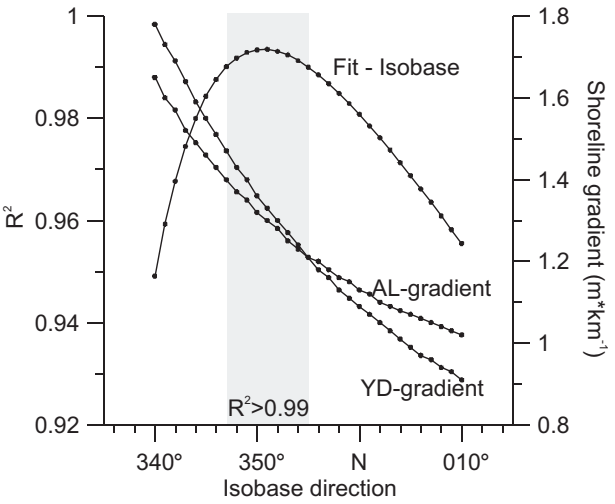

Fig. 10. Graph showing the coefficient of determination (R^2) of the linear trend surface calculated from the YD observations for different isobase directions. The interval of best fits (R^2>0.99) are illustrated by grey shading and centred at the best-fit value obtained for isobase direction of 351º. Calculated shoreline gradients are shown for both the YD and the Allerød shorelines. The best-fit isobase directions obtained shoreline gradients where the YD and Allerød shorelines both are in the range of 1.2-1.4 m km^{-1}, but may indicate a slightly steeper gradient for the YD.

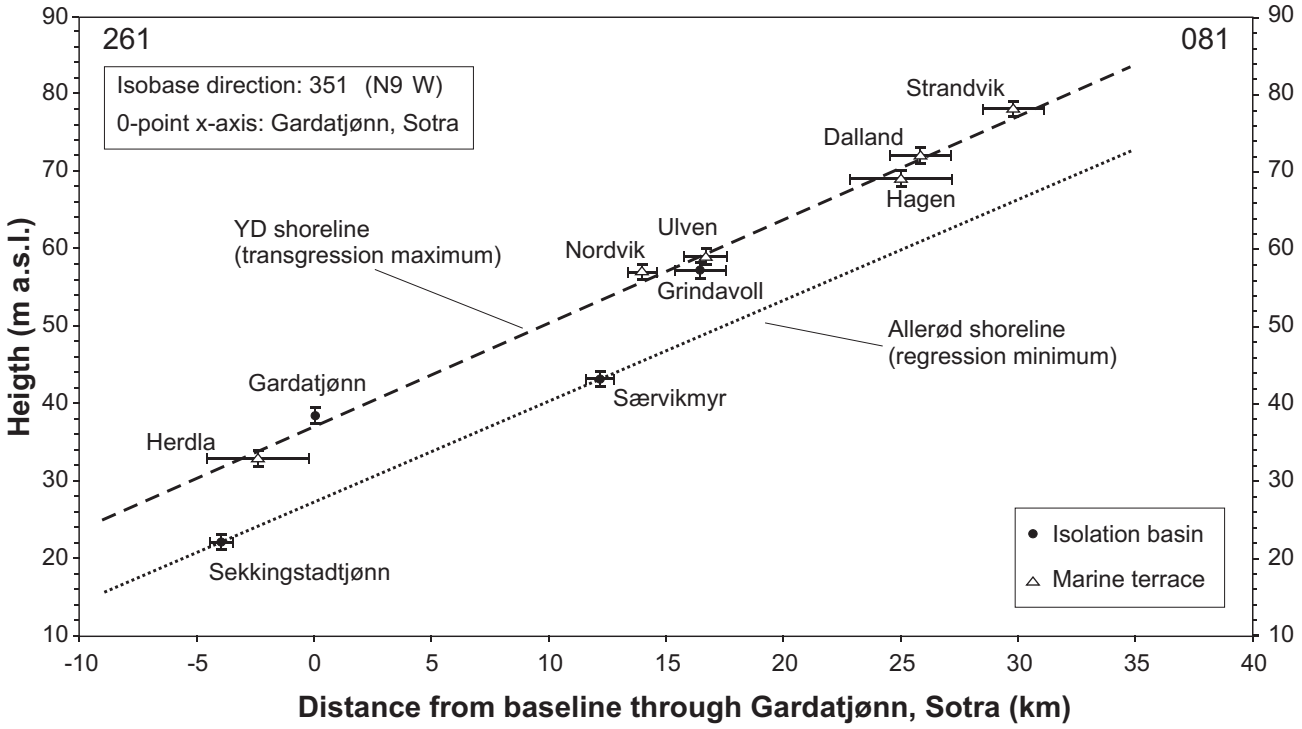

Fig. 11. Shoreline diagram for the coastal area of Hordaland constructed along a projection plane through the site Gardatjønn (Fig. 1). The diagram shows shorelines for the YD transgression maximum and the Allerød regression minimum. The YD shoreline is reconstructed by linear regression of the observations and shows a tilt of 1.33 m km^{-1} (R^2= 0.9935). The two observations of the Allerød shoreline indicate a tilt of 1.30 m km^{-1}.The diagram is constructed perpendicular to the isobase direction (351°), and the observations are projected along the isobases. Horizontal intervals indicate positions at the projection plane according to uncertainties in isobase directions of 351±4º. The observations are adjusted to show mean sea level, by subtracting 0.85 m from the height of the isolation basins and by adding 1 m to the marine terraces (see text). Note that the terrace at Dalland originally was levelled to a datum at high tide (Kolderup, 1908), and is adjusted accordingly.

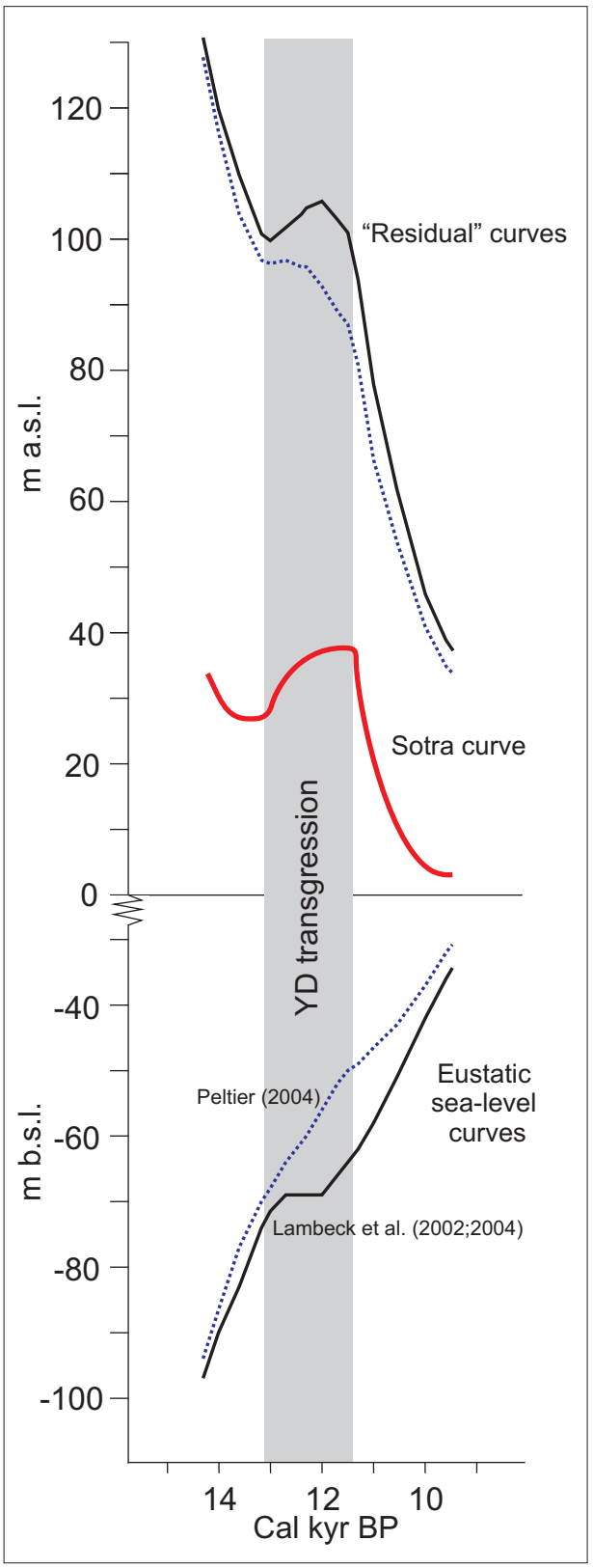

Fig. 12. The lower panel shows the estimated glacio eustatic sea-level curves, and above it, the Sotra relative sea-level curve. The uppermost panel shows the "residual" curves are constructed by subtracting the eustatic curves from the Sotra curve. Different versions of the glacio eustatic sea-level curves occur. Here we have used the curves by Lambeck et al. (2002; 2004) (black solid line and observations), and by Peltier (2004) (blue dotted line). The grey bar indicates the period of the YD transgression at Sotra.

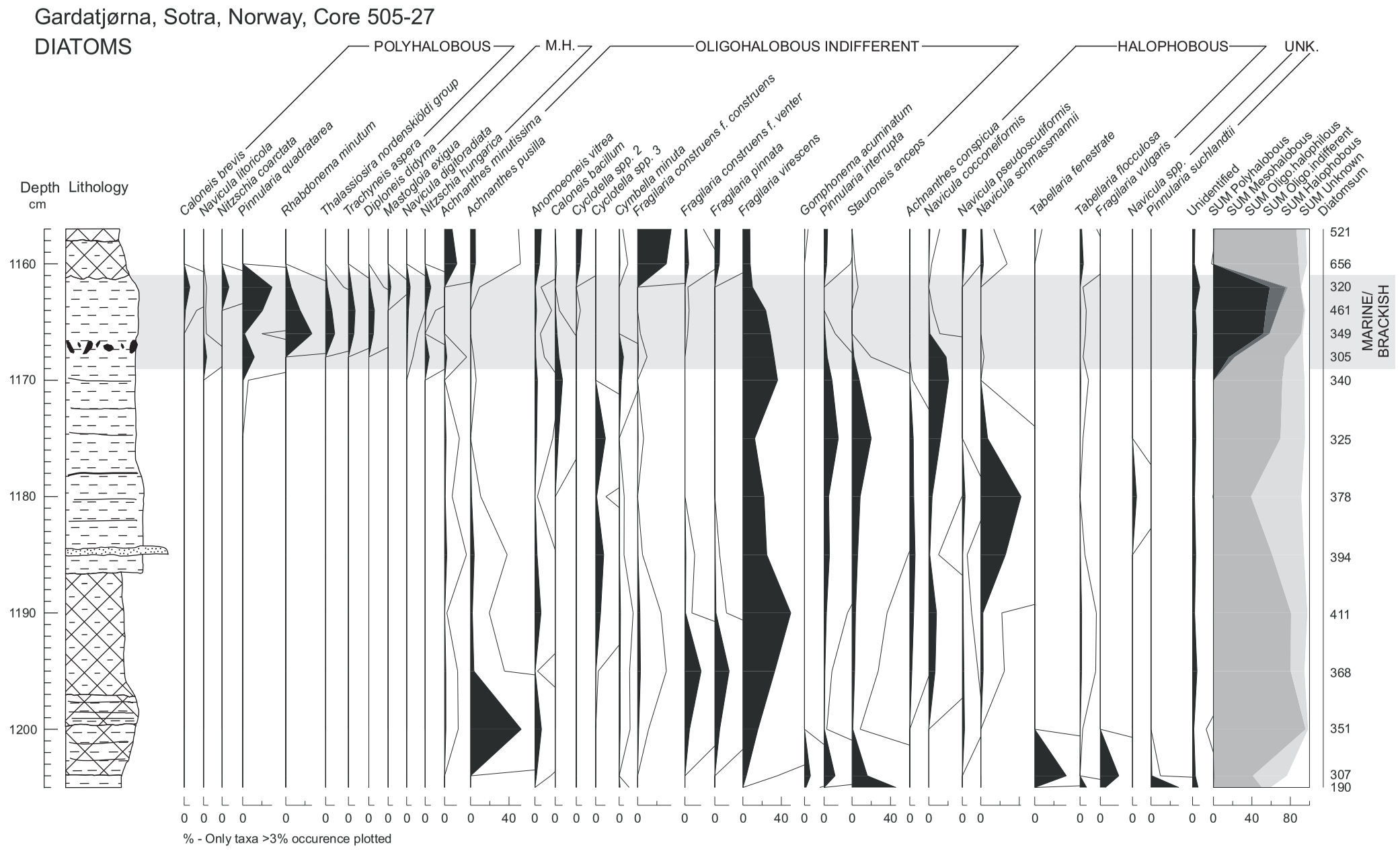
Gardatjørna, Sotra, Norway, Core 505-27
DIATOMS
POLYHALOBOUS
M.H.
OLIGOHALOBOUS INDIFFERENT
HALOPHOBOUS
UNK.
Caloneis brevis
Navicula litoricola
Nitzschia coarctata
Pinnularia quadratarea
Rhabdonema minutum
Thalassiosira nordenskiöldi group
Trachyneis aspera
Diploneis didyma
Mastogloia exigua
Navicula digitoradiata
Nitzschia hungarica
Achnanthes minutissima
Achnanthes pusilla
Anomoeoneis vitrea
Caloneis bacillum
Cyclotella spp. 2
Cyclotella spp. 3
Cymbella minuta
Fragilaria construens f. construens
Fragilaria construens f. venter
Fragilaria pinnata
Fragilaria virescens
Gomphonema acuminatum
Pinnularia interrupta
Stauroneis anceps
Achnanthes conspicua
Navicula cocconeiformis
Navicula pseudoscutiformis
Navicula schmassmannii
Tabellaria fenestrata
Tabellaria flocculosa
Fragilaria vulgaris
Navicula spp.
Pinnularia suchlandtii
Unidentified
SUM Polyhalobous
SUM Mesohalobous
SUM Oligo.halophilous
SUM Oligo.indifferent
SUM Halophobous
SUM Unknown
Diatomsum
Depth cm
Lithology
1160
1170
1180
1190
1200
521
656
320
461
349
305
340
325
378
394
411
368
351
307
190
MARINE/ BRACKISH
0 0 0 0 0 0 0 0 0 0 0 0 0 40 0 0 0 0 0 0 0 0 0 0 40 0 0 0 40 0 0 0 0 0 0 0 0 0 0 0 0 40 80
% - Only taxa >3% occurence plotted

Appendix A

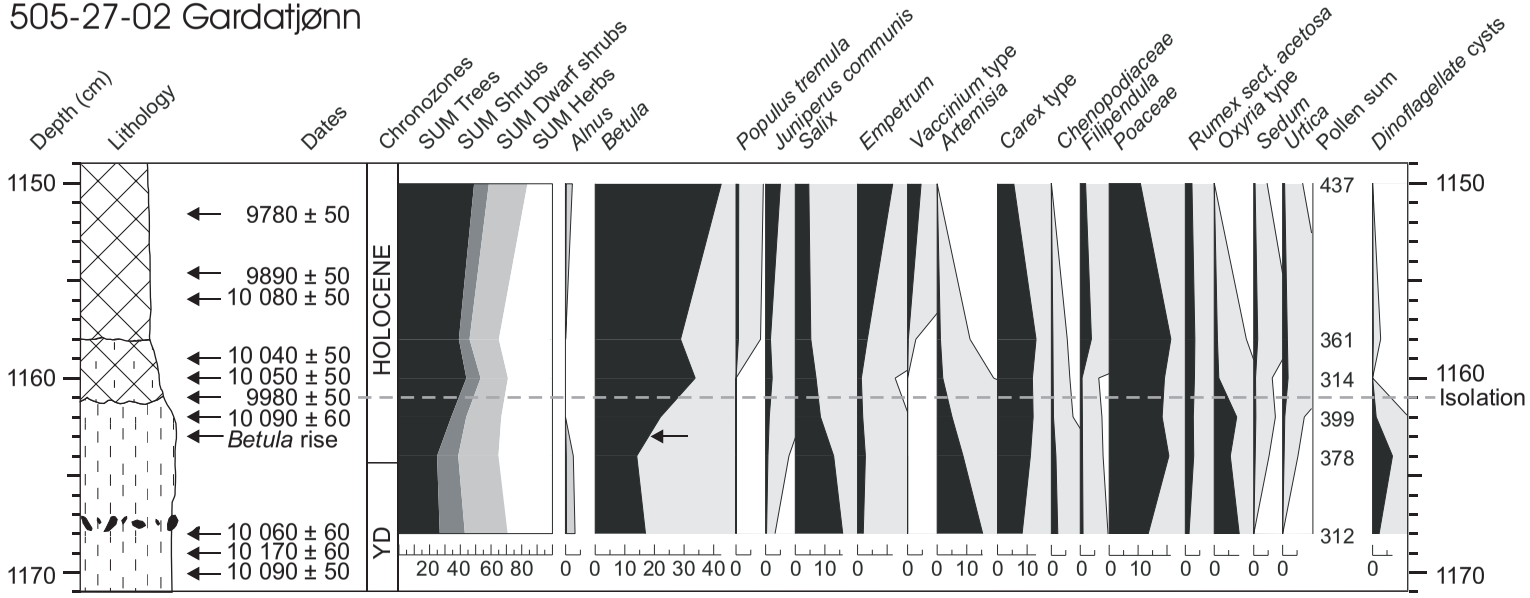
505-27-02 Gardatjønn
Depth (cm)
Lithology
Dates
Chronozones
SUM Trees
SUM Shrubs
SUM Dwarf shrubs
SUM Herbs
Alnus
Betula
Populus tremula
Juniperus communis
Salix
Empetrum
Vaccinium type
Artemisia
Carex type
Chenopodiaceae
Filipendula
Poaceae
Rumex sect. acetosa
Oxyria type
Sedum
Urtica
Pollen sum
Dinoflagellate cysts
1150
1160
1170
9780 ± 50
9890 ± 50
10 080 ± 50
10 040 ± 50
10 050 ± 50
9980 ± 50
10 090 ± 60
Betula rise
10 060 ± 60
10 170 ± 60
10 090 ± 50
HOLOCENE
YD
437
361
314
399
378
312
Isolation
20 40 60 80
0 0 10 20 30 40
0 0 0 10 0
0 0 10 0 10
0 0 0 10
0 0 0 0
0

Appendix B

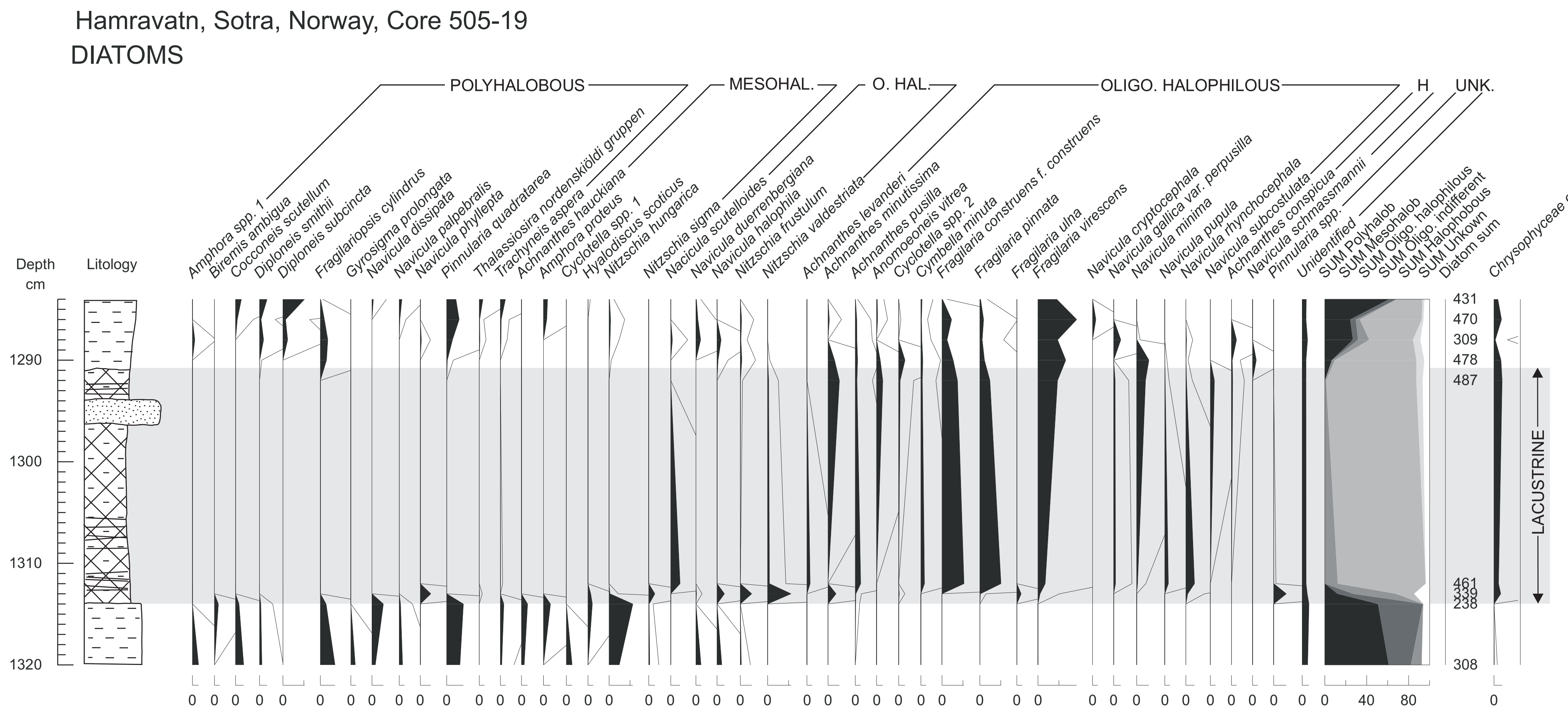

% - Only taxa >3% occurence plotted

Appendix C

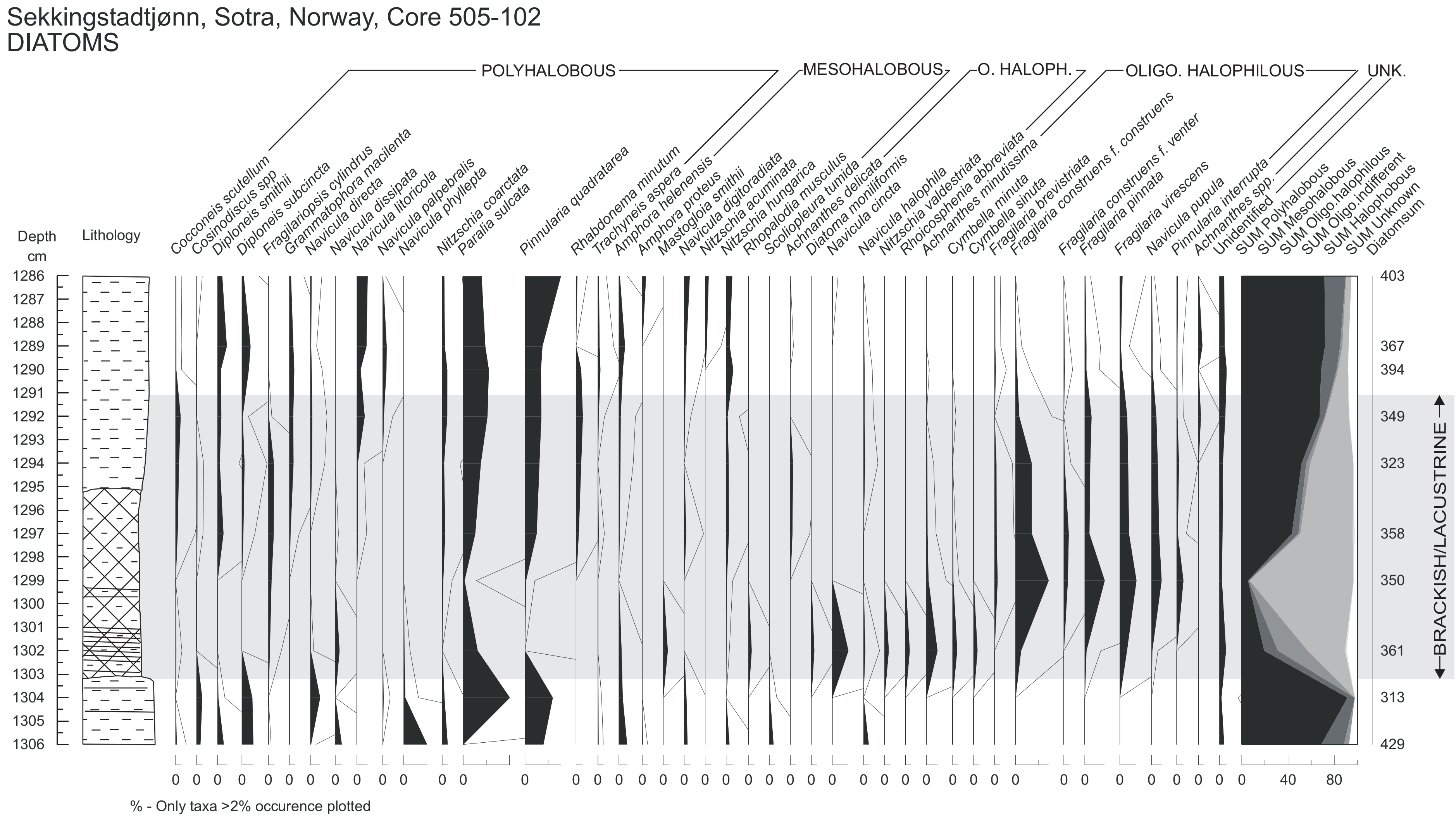
Sekkingstadtjønn, Sotra, Norway, Core 505-102
DIATOMS
POLYHALOBOUS
MESOHALOBOUS
O. HALOPH.
OLIGO. HALOPHILOUS
UNK.
Depth cm
Lithology
Cocconeis scutellum
Cosinodiscus spp
Diploneis smithii
Diploneis subcincta
Fragilariopsis cylindrus
Grammatophora macilenta
Navicula directa
Navicula dissipata
Navicula litoricola
Navicula palpebralis
Navicula phyllepta
Nitzschia coarctata
Paralia sulcata
Pinnularia quadratarea
Rhabdonema minutum
Trachyneis aspera
Amphora helenensis
Amphora proteus
Mastogloia smithii
Navicula digitoradiata
Nitzschia acuminata
Nitzschia hungarica
Rhopalodia musculus
Scoliopleura tumida
Achnanthes delicata
Diatoma moniliformis
Navicula cincta
Navicula halophila
Nitzschia valdestriata
Rhoicosphenia abbreviata
Achnanthes minutissima
Cymbella minuta
Cymbella sinuta
Fragilaria brevistriata
Fragilaria construens f. construens
Fragilaria construens f. venter
Fragilaria pinnata
Fragilaria virescens
Navicula pupula
Pinnularia interrupta
Achnanthes spp.
Unidentified
SUM Polyhalobous
SUM Mesohalobous
SUM Oligo.halophilous
SUM Oligo.indifferent
SUM Halophobous
SUM Unknown
Diatomsum
1286
1287
1288
1289
1290
1291
1292
1293
1294
1295
1296
1297
1298
1299
1300
1301
1302
1303
1304
1305
1306
403
367
394
349
323
358
350
361
313
429
BRACKISH/LACUSTRINE
0
40
80
% - Only taxa >2% occurence plotted

Appendix D